



Research paper

Discovery of potent small molecule PROTACs targeting mutant EGFR

Hong-Yi Zhao^a, Xue-Yan Yang^a, Hao Lei^a, Xiao-Xiao Xi^a, She-Min Lu^b, Jun-Jie Zhang^c,
Minhang Xin^{a,*}, San-Qi Zhang^{a,**}

^a Department of Medicinal Chemistry, School of Pharmacy, Xi'an Jiaotong University, Xi'an, Shaanxi, 710061, PR China

^b School of Basic Medical Sciences, Xi'an Jiaotong University Health Science Center, Xi'an, Shaanxi, 710061, PR China

^c School of Science, Xi'an Jiaotong University, Xi'an, Shaanxi, 710049, PR China

ARTICLE INFO

Article history:

Received 25 July 2020

Received in revised form

20 August 2020

Accepted 21 August 2020

Available online 26 August 2020

Keywords:

EGFR

PROTAC

Degradation

Autophagy

ABSTRACT

Epidermal growth factor receptor (EGFR) is an important therapeutic target for the treatment of non-small cell lung cancer. A number of efficacious EGFR tyrosine kinase inhibitors have been developed. However, acquired drug resistance largely encumbered their clinical practicability. Therefore, there is an urgent need to develop new therapeutic regime. Herein, we designed and synthesized a set of EGFR-targeting small molecule PROTACs which showed promising efficacy. In particular, VHL-recruiting compound **P3** showed potent anti-proliferative activity against HCC827 and H1975 cell lines with IC₅₀ values of 0.83 and 203.01 nM, respectively. Furthermore, both EGFR^{del19} and EGFR^{L858R/T790M} could be significantly induced to be degraded under treatment of **P3** with DC₅₀ values of 0.51 and 126.2 nM, respectively. Compound **P3** was able to dramatically suppress EGFR pathway signal transduction. Moreover, compound **P3** could significantly induce cell apoptosis, arrest cell cycle and suppress cell colony formation. In addition, we identified that ubiquitination was indispensable in the degradation process, and found that the degradation was related to autophagy. Our work would provide an alternative approach for development of potentially effective EGFR degraders and give a new clue for investigation of PROTAC-induced protein degradation.

© 2020 Elsevier Masson SAS. All rights reserved.

1. Introduction

Non-small cell lung cancer (NSCLC), one of the most aggressive cancers, is closely related to aberrant EGFR signaling, which made small molecular EGFR inhibitors exceedingly attractive for anticancer-drug development. To date, a panel of small molecular inhibitors has been discovered, and some have achieved remarkable antitumor efficacy. Gefitinib is a first-generation EGFR tyrosine kinase inhibitor (EGFR-TKI) targeting activating mutant EGFR, and affords dramatically clinical benefit [1]. Unfortunately, acquired resistance develops after short-term treatment [2]. To overcome the drug resistance caused by T790 M mutation of EGFR-TK, second-generation and third-generation EGFR-TKIs such as afatinib and osimertinib (AZD9291) have been developed [3]. However, new acquired drug resistance has been identified such as EGFR C797S mutation [4–7]. In this regard, the fourth-generation EGFR-

TKI has been exploited for EGFR C797S mutation-driven resistance. However, development of new generation of EGFR-TKI is confronted with great challenge due to the continuously heterogeneous mutations. Therefore, it is required to explore new therapies for complete treatment of NSCLC.

Recent years have witnessed tremendous advance of PROTAC (PROteolysis TARgeting Chimera) induced protein degradation. PROTAC, capable of inducing protein degradation, is a bifunctional molecule consisting of two linker-combined warheads as recruiting elements for E3 ligase and targeted protein. The distinct mechanism, which is different from kinase inhibitor, confers PROTAC potential of excelling at overcoming drug-resistance, targeting undruggable protein, and working with low dose-dependent toxicity [8–13]. Since Crews group described the notion of PROTAC through an elegant work of artificial manipulation of UPS (Ubiquitin-Proteasome System) for METAP2 degradation in 2001 [14], many different kinds of proteins have been targeted by small molecules for destruction, and the number of different PROTACs has boomed. Proteins like BET family [15–22], CDK [23–25], ALK [26,27], etc. [10,28–36] have been validated to be arrested and destroyed by small molecule PROTACs. Importantly, the androgen

* Corresponding author.

** Corresponding author.

E-mail addresses: xmhcpu@163.com (M. Xin), sqzhang@xjtu.edu.cn (S.-Q. Zhang).

receptor targeting PROTAC ARV-110 has been shown with significant efficacy in the clinical trials for treatment of patients suffering from metastatic castrate-resistant prostate cancer following enzalutamide or abiraterone, which fueled the development of PROTACs [37].

Recently, EGFR-targeting PROTACs were exploited for treatment of NSCLC based on the consideration of their therapeutic potential for solving drug resistance and their advantages over EGFR-TKI. Crews group synthesized several PROTACs (Fig. 1A and B) targeting EGFR for destruction based on the first or second-generation EGFR-TKI in 2018 [38]. Jin group also designed gefitinib-based PROTAC (Fig. 1C) [39]. Very recently, Ding group reported their work on EGFR^{L858R/T790M}-targeting PROTAC (Fig. 1D) displaying nanomolar DC₅₀ against EGFR^{L858R/T790M} and submicromolar anti-proliferative activity against H1975 cell line [40]. Our laboratory also reported EGFR-targeting PROTAC based on fourth-generation EGFR-TKI (Fig. 1E) [41]. However, although pioneer EGFR-targeting PROTACs were investigated, those PROTACs still have some defects such as no effect on double mutant EGFR or poor anti-proliferative activity.

In this study, we designed a set of EGFR-targeting small molecule PROTACs by combining a reversible EGFR-TKI with purine scaffold and CRBN or VHL ligand. These small molecule PROTACs showed potent anti-proliferative activity against HCC827 and H1975 cell lines and excellent activity of inducing mutant EGFR degradation. More importantly, we also reported that EGFR degradation induced by PROTAC was related to autophagy pathway for the first time.

2. Results and discussions

2.1. Design and synthesis of EGFR-targeting PROTACs

It was reported that purine-containing derivatives showed effective inhibitory activity against EGFR-TK [42–45]. In particular, compound **F** (Fig. 2) was discovered as a highly potent EGFR-TKI which was considered as an ideal EGFR-binding module for the design of EGFR-targeting PROTAC [42]. Therefore, in this paper, we

introduced lenalidomide (CRBN ligand, Fig. 2B) or **VHL-L** (VHL ligand, Fig. 2B) to the solvent-exposed terminal piperazine ring of compound **F** by different linkers to design a set of EGFR-targeting PROTACs, and investigated their ability of inducing EGFR degradation, antitumor activity and mechanism of action (Fig. 2).

The synthesis of target compounds was depicted in Scheme 1, 2 and 3. Scheme 1 shows synthetic route of the key intermediate **6**. Initially, commercially available 2,4-dichloro-5-nitropyrimidine (**1**) underwent nucleophilic substitution reaction with cyclopentylamine to afford compound **2** which was subsequently reacted with *tert*-butyl 4-(4-aminophenyl) piperazine-1-carboxylate to afford compound **3**. Then, reduction of **3** by catalytic hydrogenation gave compound **4** underwent cyclization reaction to generate **5** followed by deprotection employing TFA to release the key intermediate **6**.

The synthetic routes of target compounds **P1–P4** were outlined in Scheme 2. The reaction between **6** and ethyl 7-bromoheptanoate produced **7** which was subsequently converted to **8** via hydrolysis. Then, compounds **P1** and **P3** were obtained through acylation reaction of **8** with lenalidomide and **VHL-L**, respectively. Lenalidomide or **VHL-L** was transformed to **9a** or **9b** via acylation with 8-bromooctanoic acid. **P2** or **P4** was generated from **9a** or **9b** through nucleophilic substitution with intermediate **6**.

Compounds **P5–P10** with different polyethylene glycol linkers were synthesized according to Scheme 3. Intermediate **6** reacted with polyethylene glycol di-*p*-toluenesulfonate to produce **11a–11c** which were converted to **12a–12c** via nucleophilic substitution with **10**. Subsequently, deprotection of **12a–12c** followed by acylation with lenalidomide generated target compounds **P5–P7**. Reaction of polyethylene glycol di-*p*-toluenesulfonate with **VHL-L** gave intermediate **13a–13c**. Finally, **P8–P10** were obtained from **13a–13c** via nucleophilic substitution with **6**. Thus, we synthesized ten target compounds with different linkers and E3-recruiting elements.

2.2. Evaluation of the anti-proliferative activity in vitro

With target compounds in hand, we firstly evaluated their anti-proliferative activity against HCC827 cell line (Table 1 and Fig. S1).

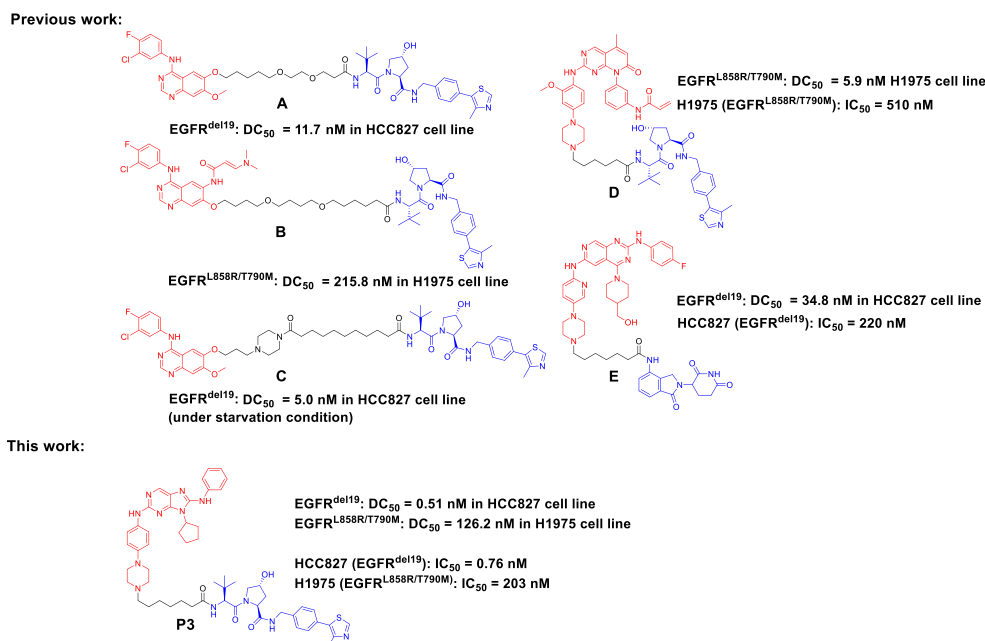


Fig. 1. Structures of EGFR-targeting PROTACs and their activity profiles.

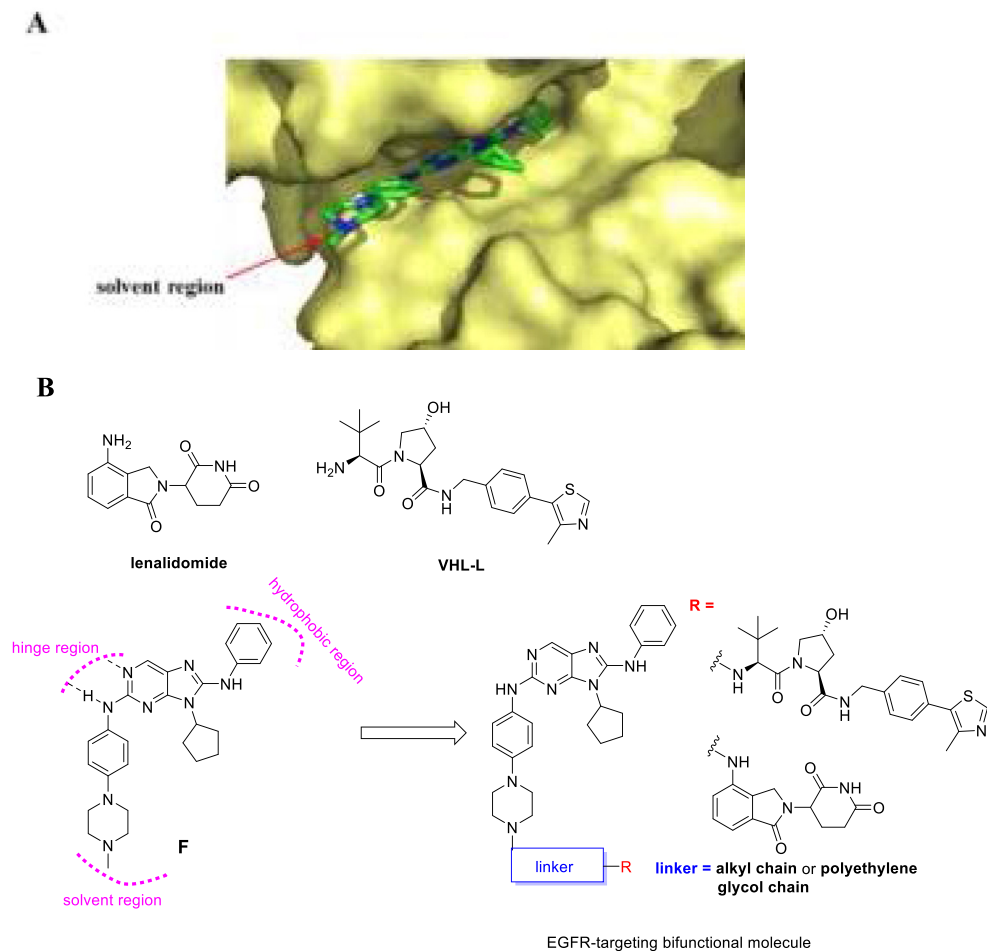
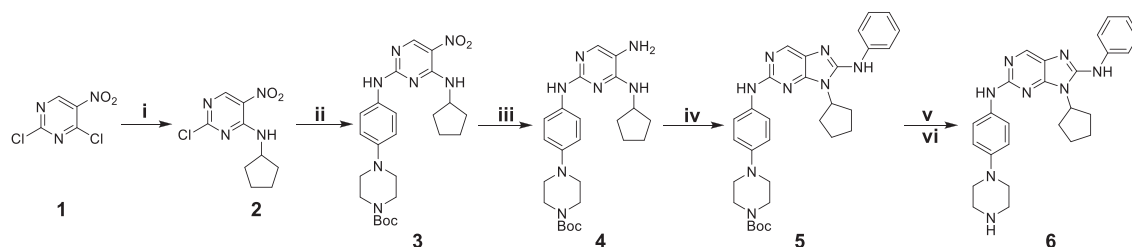


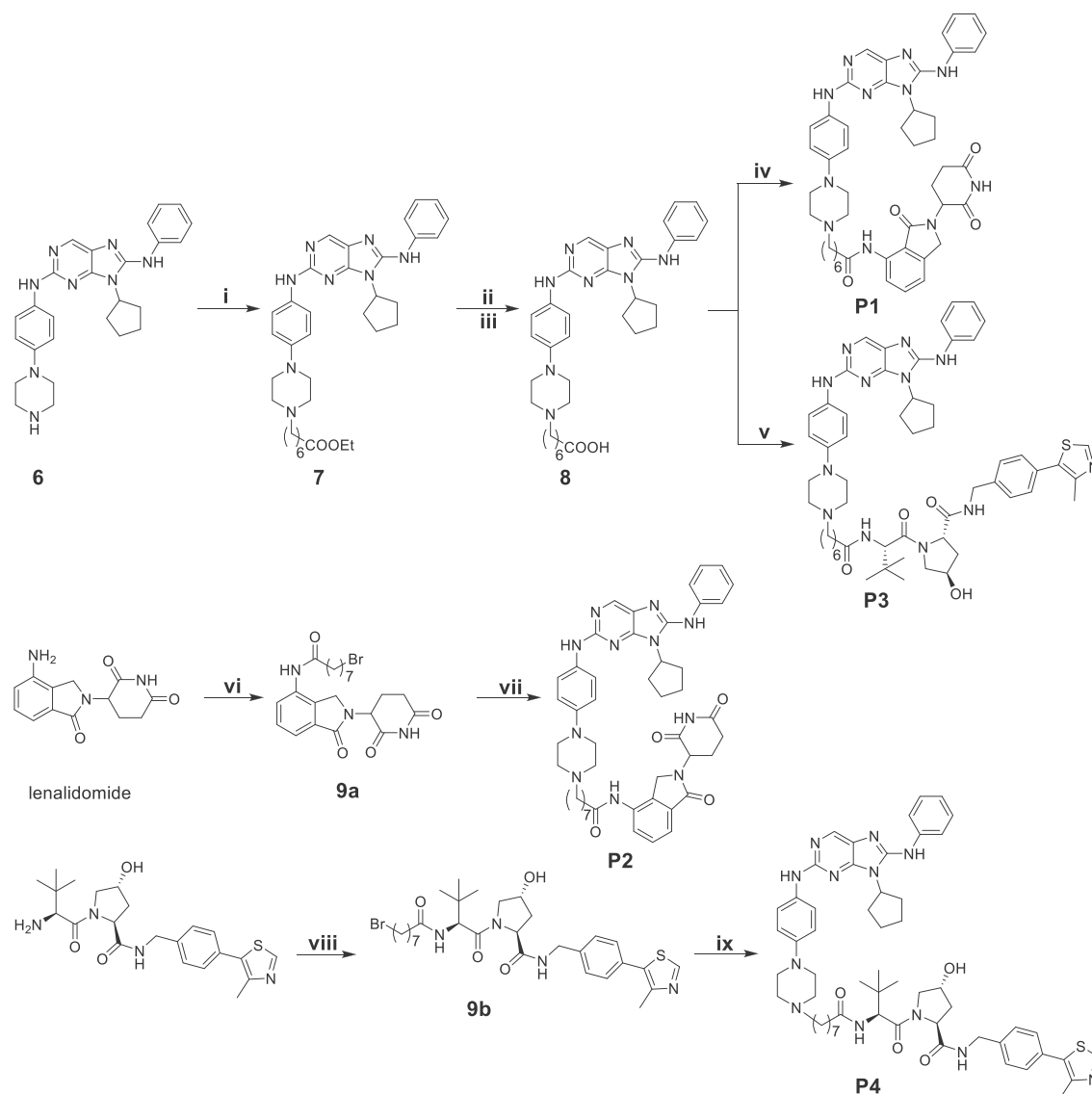
Fig. 2. (A) Docking of compound **F** with EGFR (PDB: 3IKA) using Sybyl-X 2.0. (B) Design of EGFR-targeting small molecule PROTAC.



Scheme 1. Synthesis of key intermediate **6**. Reagents and reaction conditions: (i) cyclopentylamine, TEA, DCM, $-20\text{ }^{\circ}\text{C}$ ~ rt, 80%; (ii) *tert*-butyl 4-(4-aminophenyl) piperazine-1-carboxylate, Na_2CO_3 , EtOH, rt, 88%; (iii) Pd/C, H_2 , MeOH, $50\text{ }^{\circ}\text{C}$, 94%; (iv) phenyl isothiocyanate, EDCl, DIPEA, 1,2-dichloroethane, $60\text{ }^{\circ}\text{C}$, 92%; (v) DCM, TFA, rt; (vi) saturated Na_2CO_3 (aq), 90% overall yield.

Compound **F** and AZD9291 were used as positive controls. As illustrated in Table 1, compounds **P1–P7** dominantly inhibited growth of HCC827 cell line, which was comparable to AZD9291 and parent compound **F**. Among them, compounds with alkyl linker and **VHL-L** components (**P3–P4**) were a little more effective than the others with IC_{50} values of 0.83 and 0.76 nM, respectively. Moreover, the activity of compounds with PEG linker and lenalidomide E3-recruiting element (**P1–P2**) was almost indistinguishable with that of their counterparts (**P5–P7**). Converting carbonyl-containing alkyl linker to polyethylene glycol chain resulted in the diminished activity when using **VHL-L** as E3-recruiting element (**P3–P4**, **P8–P10**). Subsequently, we tested inhibitory activity of the

compounds against H1975 cell line harboring drug-resistant mutation (L858R/T790 M). Compound **P3** displayed submicromolar inhibitory activity against H1975 ($\text{IC}_{50} = 203\text{ nM}$) which was about twice as good as that of compound **F** ($\text{IC}_{50} = 430\text{ nM}$) while the others were less effective (Table 1 and Fig. S1). Next, A431 cell line was selected to evaluate their cellular selectivity as it expressed high level of wild-type EGFR. **P1–P4** exhibited submicromolar inhibitory activity against A431 indicating good selectivity against HCC827 (Table 1 and Fig. S1). As compound **F** was reported to have significant inhibitory activity against VEGFR2 [42], we tested our compounds on HepG2 cell line. Our experiment demonstrated the synthesized compounds were almost ineffective on HepG2 cell line



Scheme 2. Synthesis of target compounds **P1–P4**. Reagents and reaction conditions: (i) Br(CH₂)₆COOEt, K₂CO₃, KI, DMF, 60 °C, 50%; (ii) NaOH, EtOH, H₂O, rt; (iii) 1 M HCl, 79% overall yield; (iv) lenalidomide, HATU, DIPEA, DMF, rt, 51%; (v) **VHL-L**, HATU, DIPEA, DMF, rt, 51%; (vi) Br(CH₂)₇COOH, EDCI, DMF, 40 °C, 35%; (vii) **6**, DIPEA, KI, NMP, 100 °C, 26%; (viii) Br(CH₂)₇COOH, HATU, DIPEA, DCM, rt, 83%; (ix) **6**, K₂CO₃, KI, CH₃CN, reflux, 63%.

indicating their high selectivity against lung cancer cells. These results indicated that the composition of linker had negligible impact on anti-proliferative activity when using lenalidomide as E3-recruiting element, and that the PROTACs decorated with VHL ligand were more responsive to EGFR^{L858R/T790M} than those with CRBN ligand.

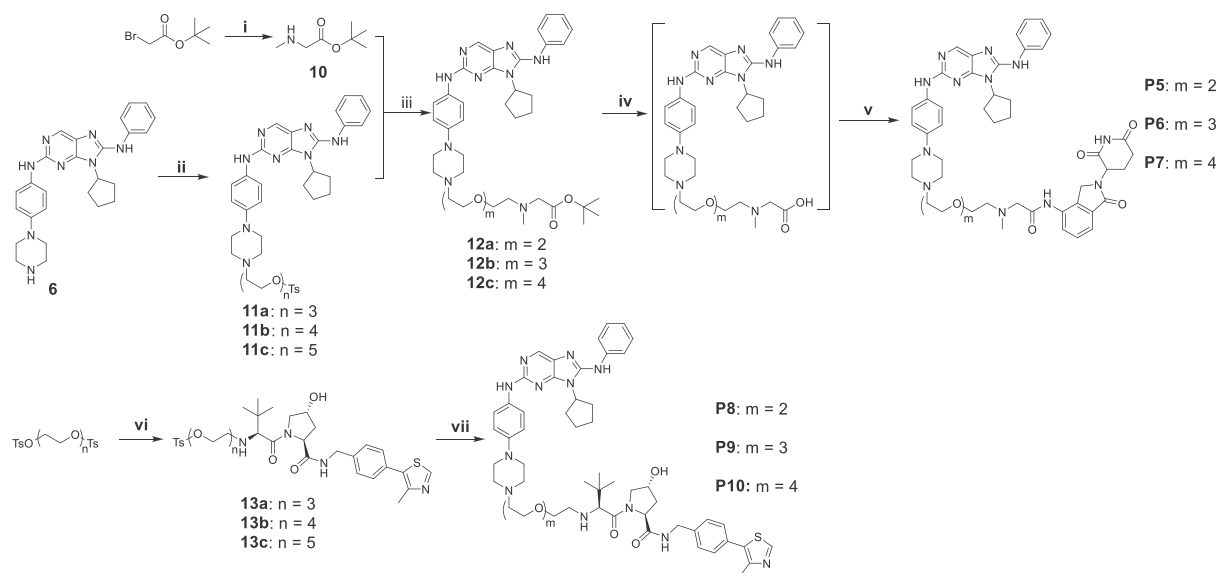
2.3. PROTAC-induced EGFR degradation

Having determined anti-proliferative activity of the compounds against tumor cells, we evaluated their capability of inducing EGFR degradation (Fig. 3A). Obviously, compounds **P1–P7** with different linkers or E3-recruiting elements were able to mediate EGFR degradation. Treatment at the concentration of 333 nM impaired the activity because of hook effect. However, compounds **P8–P10** were barely incompetent in inducing EGFR degradation, which is consistent with their cellular activity. Based on both cellular and degradative activity, we selected compounds **P3**, **P4** and **P6** for further study.

Induced EGFR degradation was time-dependent as shown in Fig. 3B. The maximum effect of the compounds was achieved almost after 48 h. Furthermore, **P3**, **P4** and **P6** all displayed excellent activity of inducing EGFR^{del19} degradation with nanomolar DC₅₀ values of 0.51, 3.54 and 1.91 nM, respectively, while their parental compound **F** was ineffective at the concentration of 100 nM (Fig. 3C and D).

It remains a challenge to develop effective EGFR^{L858R/T790M}-targeting PROTAC. Then the induced EGFR degradation in H1975 cell line was studied. As shown in Fig. 4, **P3** and its analogue **P4** were responsive to double mutant EGFR in H1975 cell line (DC₅₀ = 126.2 and 151.2 nM, respectively. D_{max} = 90.3% and 80.3%, respectively. Fig. 4A and C). Additionally, almost no degradation on wild-type EGFR (EGFR^{WT}) was examined in A431 cell line under treatment of **P3** or **P6** indicating its excellent selectivity (Fig. 4B and Fig. S2).

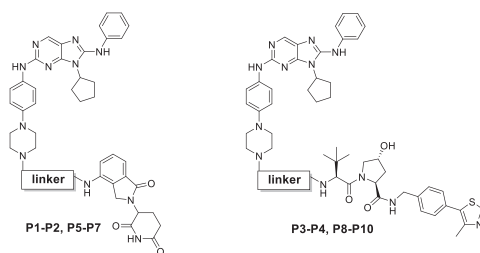
Subsequently, we determined duration time of their effect. After being washed out for 24 h, **P3** and **P4** still suppressed EGFR level in HCC827 cell line, which was more long-lasting than the effect of CRBN-recruiting **P6** (Fig. 5A). Furthermore, EGFR level almost



Scheme 3. Synthesis of target compounds **P5–P10**. Reagents and reaction conditions: (i) methylamine, CH₃CN, 0 °C ~ rt, 46%; (ii) TsO(CH₂CH₂O)_nTs, CH₃CN, K₂CO₃, 60 °C, 22–36%; (iii) CH₃CN, K₂CO₃, reflux, 36–68%; (iv) TFA, DCM; (v) lenalidomide, HATU, DIPEA, DMF, rt, 28%–31%; (vi) **VHL-L**, CH₃CN, K₂CO₃, 60 °C, 25–35%; (vii) **6**, K₂CO₃, CH₃CN, reflux, 28–57%.

Table 1

In vitro anti-proliferative activity of compounds **P1–P10** against cancer cells (n = 3, x ± SD).



comps	Linker	IC ₅₀ (nM)			
		A431 (EGFR ^{WT})	HCC827 (EGFR ^{del19})	H1975 (EGFR ^{L858R/T790M})	HepG2 (VEGFR2)
P1		220 ± 28	1.41 ± 0.15	9301 ± 57	>5000
P2		240 ± 40	2.61 ± 1.58	3776 ± 347	>5000
P3		245 ± 30	0.83 ± 0.30	203 ± 21	>5000
P4		330 ± 35	0.76 ± 0.33	970 ± 162	>5000
P5		2667 ± 315	1.39 ± 0.23	1211 ± 140	>5000
P6		1856 ± 346	2.00 ± 0.72	3176 ± 223	>5000
P7		2723 ± 368	2.83 ± 0.38	3336 ± 460	>5000
P8		ND	53.49 ± 0.49	1100 ± 283	>5000
P9		ND	54.38 ± 3.00	2100 ± 57	>5000
P10		ND	62.00 ± 1.86	2894 ± 345	>5000
F	—	163 ± 25	0.82 ± 0.69	430 ± 85	>5000
AZD9291	—	742 ± 53	0.97 ± 0.10	42 ± 7	ND

"ND", not determined.

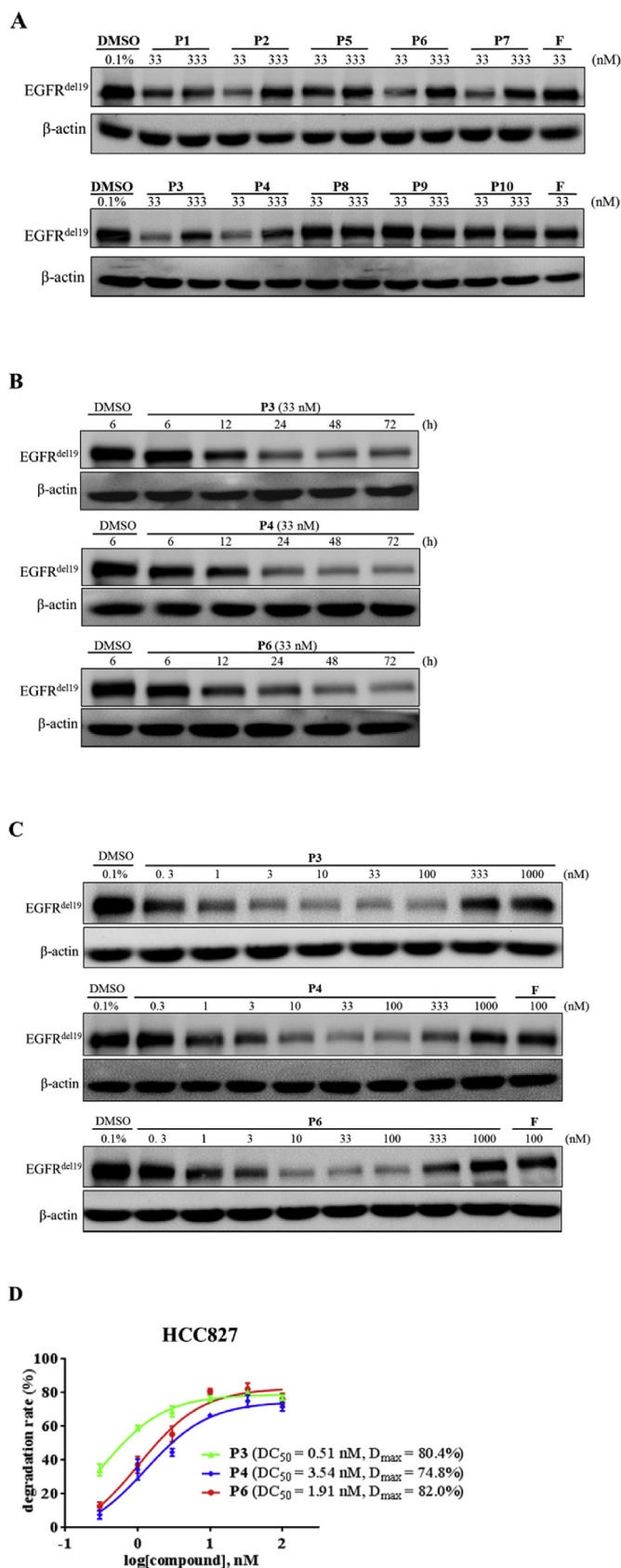


Fig. 3. PROTAC-induced EGFR^{del19} degradation in HCC827 cell line detected with Western blotting (A) The cell line was treated with compounds **P1**–**P10** with indicated concentrations for 24 h. (B) The cell line was treated with compounds **P3**, **P4** or **P6** at 33 nM, and protein was collected at each indicated time point. (C, D) The cell line was treated with **P3**, **P4** or **P6** with indicated concentrations for 48 h ($n = 3$).

recovered after 48 h whether treated with **P3** or **P6**. In contrast, double mutant EGFR (EGFR^{L858R/T790M}) level was constantly suppressed even after 48 h (Fig. 4B).

To explore the effect of the degrader on downstream signaling, we detected the level of phosphorylated EGFR and Akt in HCC827 and H1975 cell lines. As seen in Fig. 6, the phosphorylation of EGFR and its downstream effector Akt was dramatically reduced in HCC827 and H1975 cell lines when treated with **P3** at concentrations as low as 3 and 100 nM, respectively, while Akt remained intact (Fig. 6A and B). These results indicated that **P3** was able to inhibit signal transduction of EGFR pathway.

2.4. Mechanism study

UPS was reported to be involved in the PROTAC-induced protein degradation in which the formation of ternary complex (protein-PROTAC-E3) was indispensable for protein ubiquitination and subsequent split by proteasome. Therefore, we firstly inverted the hydroxyproline stereochemistry on the **VHL-L** to synthesize diastereomer **P11** (Fig. 7C) to abolish its ability to bind VHL. **P11** displayed much weaker anti-proliferative and degradative activity than **P3** indicating that VHL binding was crucial for ternary complex formation in the degradative process (Fig. 7A–C). Furthermore, as shown in Fig. 8, no degradation of EGFR was detected upon treatment of ubiquitination inhibitor MLN4924 despite the presence of CRBN-recruiting **P6** (Fig. 8A and S3A) or VHL-recruiting **P3** (Fig. 8B and S3B) implying the necessity of EGFR ubiquitination for destruction. As another evidence of ternary complex formation, EGFR-TKI **F** (Fig. 8A and B, S3A–S3B) or E3 ligands lenalidomide (Fig. 8A and S3A) was also capable of preventing EGFR degradation. Unexpectedly, **VHL-L** was unable to antagonize the effect of compound **P3** possibly due to its weak VHL-binding affinity (Fig. 8B and S3B). Subsequently, we synthesized acetylated **VHL-L**, namely, **VHL-Ac** (Fig. 8D), and discovered that **VHL-Ac** attenuated the effect of **P3** suggesting its stronger VHL-binding affinity (Fig. 8C and S3C).

Proteasome was widely supposed to be the intracellular protein-degrading machinery in the process of PROTAC-induced protein degradation. Nonetheless, proteasome inhibitor MG132 had no impact on induced EGFR destruction at concentration of 10 μ M in our research (Fig. 8A and B, S3A–S3B). This prompted us to turn our attention to autophagic-lysosomal system, another protein-hydrolyzing pathway.

We next explored the relationship between autophagy and EGFR degradation. Chloroquine, a widely used autophagy inhibitor, slightly impaired the effect of **P6** or **P3** in HCC827 cell line as well as in H1975 cell line indicating the EGFR degradation was lysosome-dependent (Figs. 8C and 9A, S3C–S3D). We supposed that the weak inhibition of chloroquine on EGFR degradation was partly due to its ability of inducing autophagy (Fig. S4). Subsequently, we devoted to exploring whether enhancement of autophagy could amplify the effect of **P3**. Serum deprivation was proved to induce autophagy, so we used medium without fetal bovine serum (FBS) to culture cells and discovered that EGFR degradation was facilitated under the starvation condition (Fig. 9B, S5A–S5B). LC3-II/I ratio and p62 level confirmed the enhancement of autophagy. Rapamycin, a mammalian target of rapamycin (mTOR) inhibitor, was also capable of inducing autophagy. As shown in Fig. 9C and S5C, rapamycin accelerated EGFR degradation in H1975 cells line. Thus, it was ensured that induced EGFR degradation initiated from protein ubiquitination upon formation of ternary complex, and that autophagic-lysosomal system was implicated in the process.

2.5. Cell apoptosis assay

We next determined whether compound **P3** could induce cell

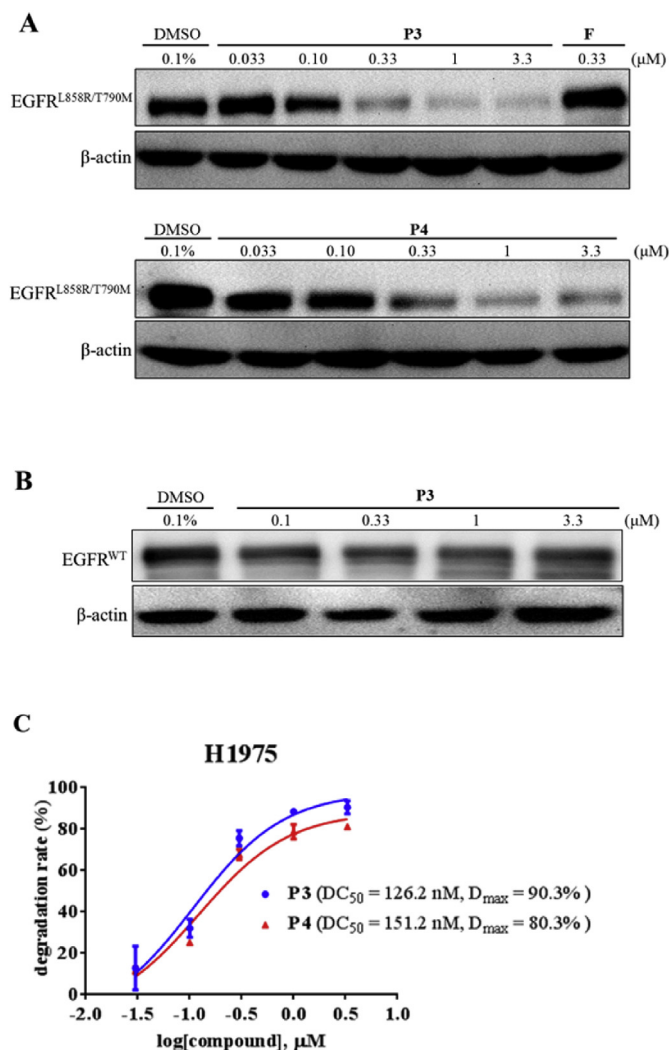


Fig. 4. PROTAC-induced EGFR degradation in H1975 (A, C) and A431 (B) cell lines detected with Western blotting. Cell lines were treated with compound **P3** or **P4** under indicated concentrations for 48 h (n = 3).

apoptosis. Compound **P3** induced 31.07% and 44.80% of HCC827 cell line to undergo apoptosis at concentration of 10 and 100 nM, respectively (Fig. 10 and S6). However, it was not competent in inducing apoptosis of H1975 cell line.

2.6. Cell cycle assay

Flow cytometry was employed to examine the impact of **P3** on cycle of tumor cells. As depicted in Fig. 11 and S7, the degrader **P3** was able to arrest both HCC827 and H1975 cell lines at G1 phase.

2.7. Colony formation assay

As shown in Fig. 12 and S8, Colony formation assay confirmed that **P3** could significantly inhibit cell cloning of HCC827 and H1975 cell lines at concentrations as low as 1 and 100 nM, respectively. These results indicated that **P3** could effectively inhibit the growth of tumor cells.

3. Conclusions

Emerging PROTAC technology displays many advantages due to

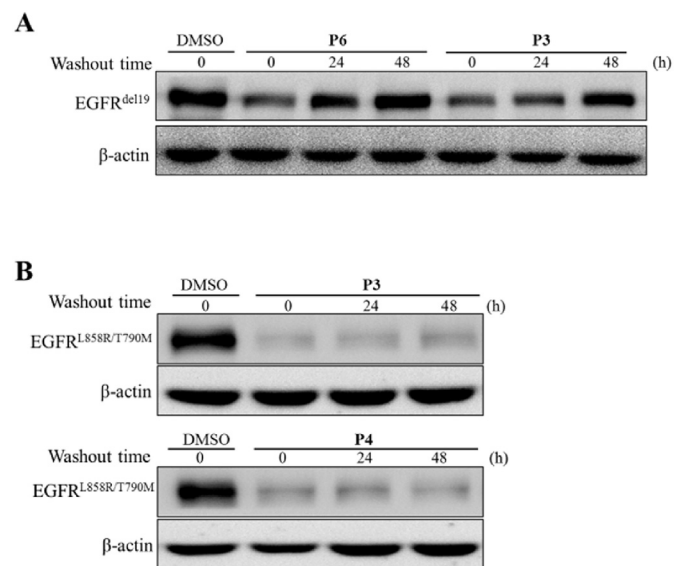


Fig. 5. Investigation of EGFR level after the compounds were removed. (A) HCC827 cell line was treated with indicated compounds (33 nM) for 24 h. (B) H1975 cell line was treated with indicated compounds (333 nM) for 48 h. Then, the medium was removed and fresh medium without compounds was added. Protein was collected after indicated time and analyzed by Western blotting (n = 2).

its different mode of action from traditional enzyme inhibitors. Although several EGFR-targeting PROTACs were developed, they suffered from no effect on double mutant EGFR or poor anti-proliferative activity. Herein, we have discovered a novel degrader (compound **P3**) capable of effectively inducing mutant EGFR degradation and dramatically suppressing the growth of HCC827 and H1975 cell lines as well as EGFR pathway signal transduction. Additionally, compound **P3** could prompt cell apoptosis, arrest cell cycle and suppress cell colony formation. We further confirmed that induced EGFR degradation initiated from protein ubiquitination upon formation of ternary complex, and reported for the first time that PROTAC-induced EGFR degradation was related to autophagy. In short, compound **P3** was finally discovered as a potent EGFR degrader and antitumor agent. Our work would provide an alternative approach for development of clinically effective EGFR degraders and give a new clue for investigation of PROTAC-induced protein degradation.

4. Experimental section

4.1. Chemistry

Unless specified otherwise, all the starting materials, reagents and solvents are commercially available. All the reactions were monitored by thin-layer chromatography on silica gel plates (GF254) and visualized with UV light (254 nm and 365 nm). NMR spectra were recorded on a 400 Bruker NMR spectrometer with tetramethylsilane (TMS) as an internal reference. All chemical shifts are reported in parts per million (ppm). The following abbreviations were used to describe peak splitting patterns when appropriate: s (singlet), d (doublet), t (triplet), m (multiplet), br (broad signal), dd (doublet of doublets). Coupling constants (J) are expressed in hertz unit (Hz). Mass spectrum (MS) was obtained by ESI-MS (Skyray instrument, LC-MS 1000). High resolution mass spectrum (HRMS) was obtained by electrospray ionization (positive mode) on an Ultra performance liquid chromatography-Quadrupole-time of flight Mass Spectrometer (WATERS I-Class VION IMS Q-TOF).

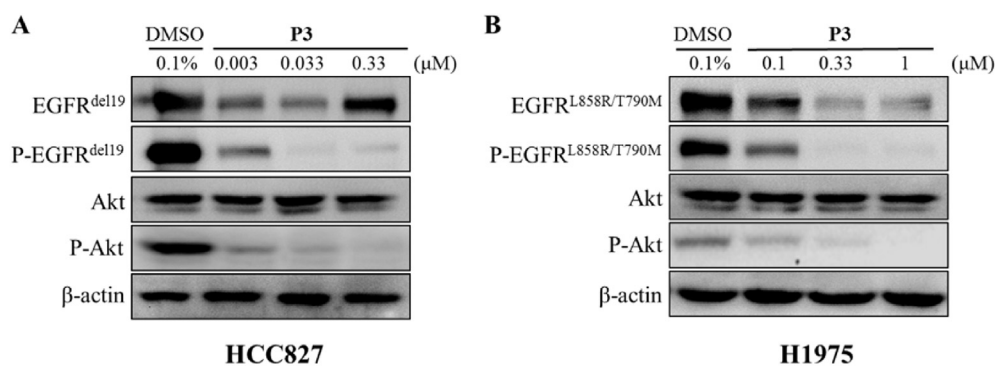


Fig. 6. P3 significantly reduced the level of phosphorylated EGFR (P-EGFR) and Akt (P-Akt). HCC827 (A) and H1975 (B) cell lines were treated with compound P3 with indicated concentrations for 48 h. The protein was collected and analyzed by Western blotting (n = 2).

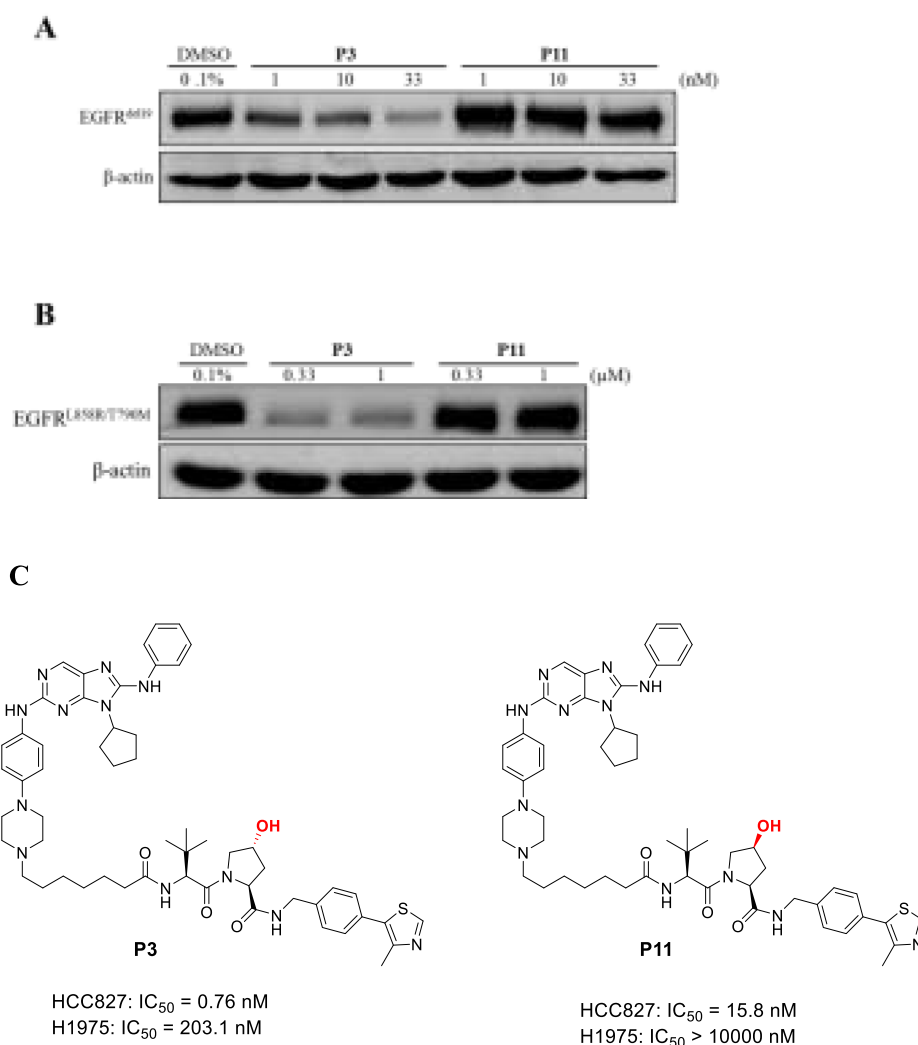


Fig. 7. HCC827 (A) or H1975 (B) cell lines were treated with P3 or its diastereomer P11 with indicated concentrations for 24 h. EGFR level was analyzed by Western blotting. (C) Chemical structure of P3 and P11. (n = 3).

4.1.1. 2-Chloro-N-cyclopentyl-5-nitropyrimidin-4-amine (2)

To a round bottom flask were added DCM (50 mL) and 2,4-dichloro-5-nitro-pyrimidine (5.00 g, 25.8 mmol). The solution was stirred at -20 °C for 10 min, and a solution of cyclopentylamine (2.42 g, 28.4 mmol) and triethylamine (3.92 g, 38.7 mmol) in DCM

(50 mL) was added dropwise. The resulted mixture was washed with water (3 × 15 mL) and saturated brine (20 mL), dried with anhydrous sodium sulfate and evaporated under vacuum to afford compound 2 without further purification. Yellow solid, 80% yield, ¹H NMR (400 MHz, CDCl₃), δ 9.03 (s, 1H), 8.39 (s, 1H), 4.60 (dd,

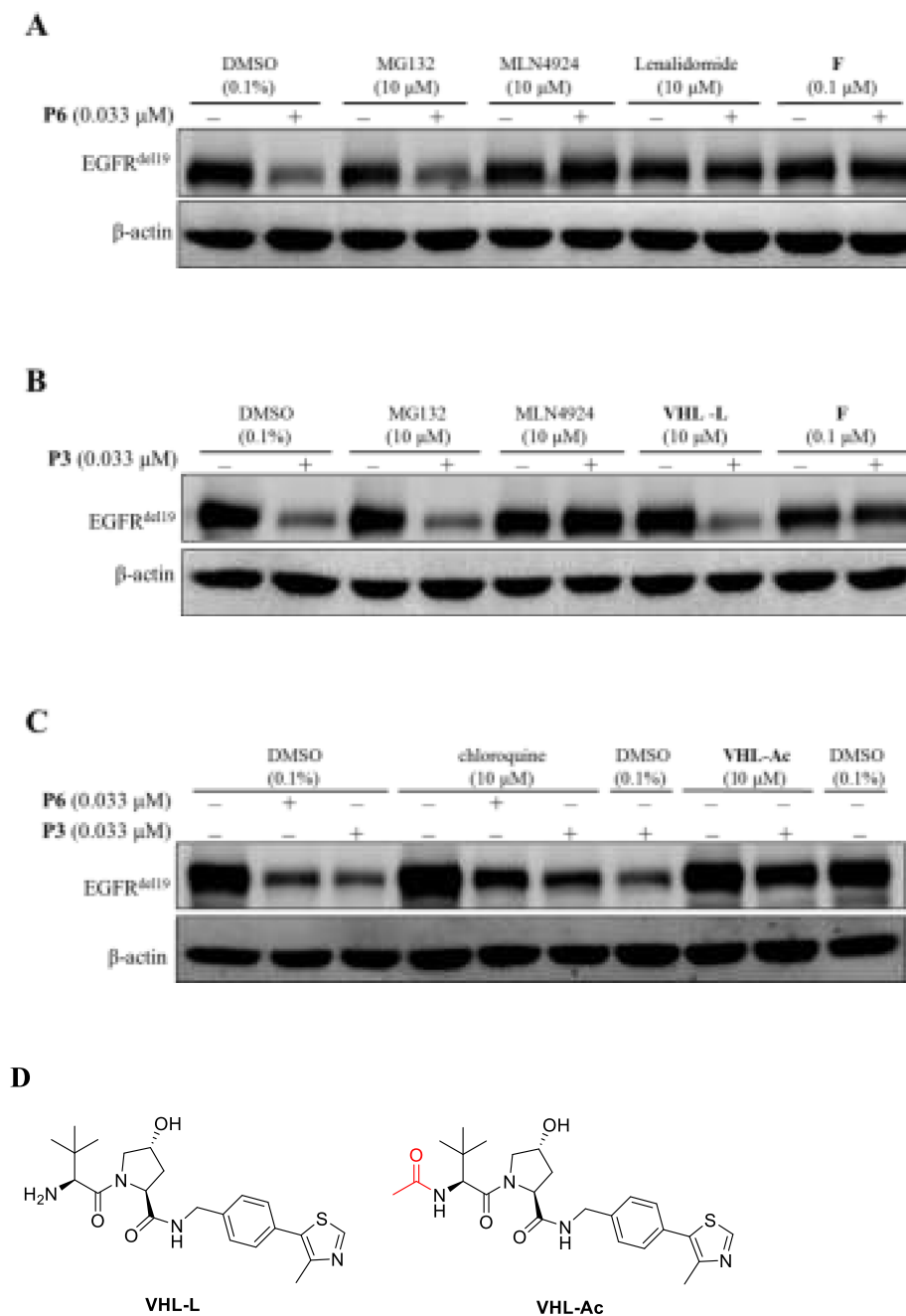


Fig. 8. Degradation mechanism investigation. HCC827 cell line was pretreated with indicated compounds or DMSO for 2 h. Then **P3** or **P6** was added. And protein was collected after 24 h and analyzed by Western blotting (A–C). (D) Chemical structures of **VHL-L** and **VHL-Ac**. (n = 3).

$J = 13.9, 6.9 \text{ Hz}, 1\text{H}$, 2.32–2.11 (m, 2H), 1.90–1.65 (m, 4H), 1.64–1.48 (m, 2H). MS (ESI): m/z calcd for $\text{C}_9\text{H}_{12}\text{ClN}_4\text{O}_2$: 243.1 $[\text{M}+\text{H}]^+$; found: 455.5.

4.1.2. *Tert-butyl 4-(4-((4-(cyclopentylamino)-5-nitropyrimidin-2-yl)amino)phenyl) piperazine-1-carboxylate (3)*

Tert-butyl 4-(4-aminophenyl)piperazine-1-carboxylate (3.82 g, 13.8 mmol) was dissolved in EtOH (25 mL). Then, Na_2CO_3 (2.19 g, 20.7 mmol) and **2** were added. The resulted mixture was stirred at room temperature overnight. The precipitated solid was filtered and washed with EtOH ($3 \times 3 \text{ mL}$). The filter cake was mixed with water (20 mL) followed by filtration to produce **3**. Yellow solid, 88%

yield, $^1\text{H NMR}$ (400 MHz, CDCl_3), δ 9.01 (s, 1H), 8.53 (s, 1H), 7.69 (s, 1H), 7.55 (s, 2H), 6.95 (d, $J = 8.8 \text{ Hz}$, 2H), 4.55–4.45 (m, 1H), 3.68–3.55 (m, 4H), 3.22–3.06 (m, 4H), 2.17–2.04 (m, 2H), 1.85–1.76 (m, 2H), 1.73–1.59 (m, 4H), 1.49 (s, 9H). MS (ESI): m/z calcd for $\text{C}_{24}\text{H}_{34}\text{N}_7\text{O}_4$: 484.3 $[\text{M}+\text{H}]^+$; found: 484.4.

4.1.3. *Tert-butyl 4-(4-((5-amino-4-(cyclopentylamino)pyrimidin-2-yl)amino)phenyl)piperazine-1-carboxylate (4)*

Compound **3** (5.00 g, 10.34 mmol) and Pd/C (1.00 g, 5%) were mixed with MeOH (70 mL). The suspension was stirred under H_2 atmosphere at 55°C overnight. The mixture was filtered through Celite, and the filtrate was evaporated under vacuum to produce

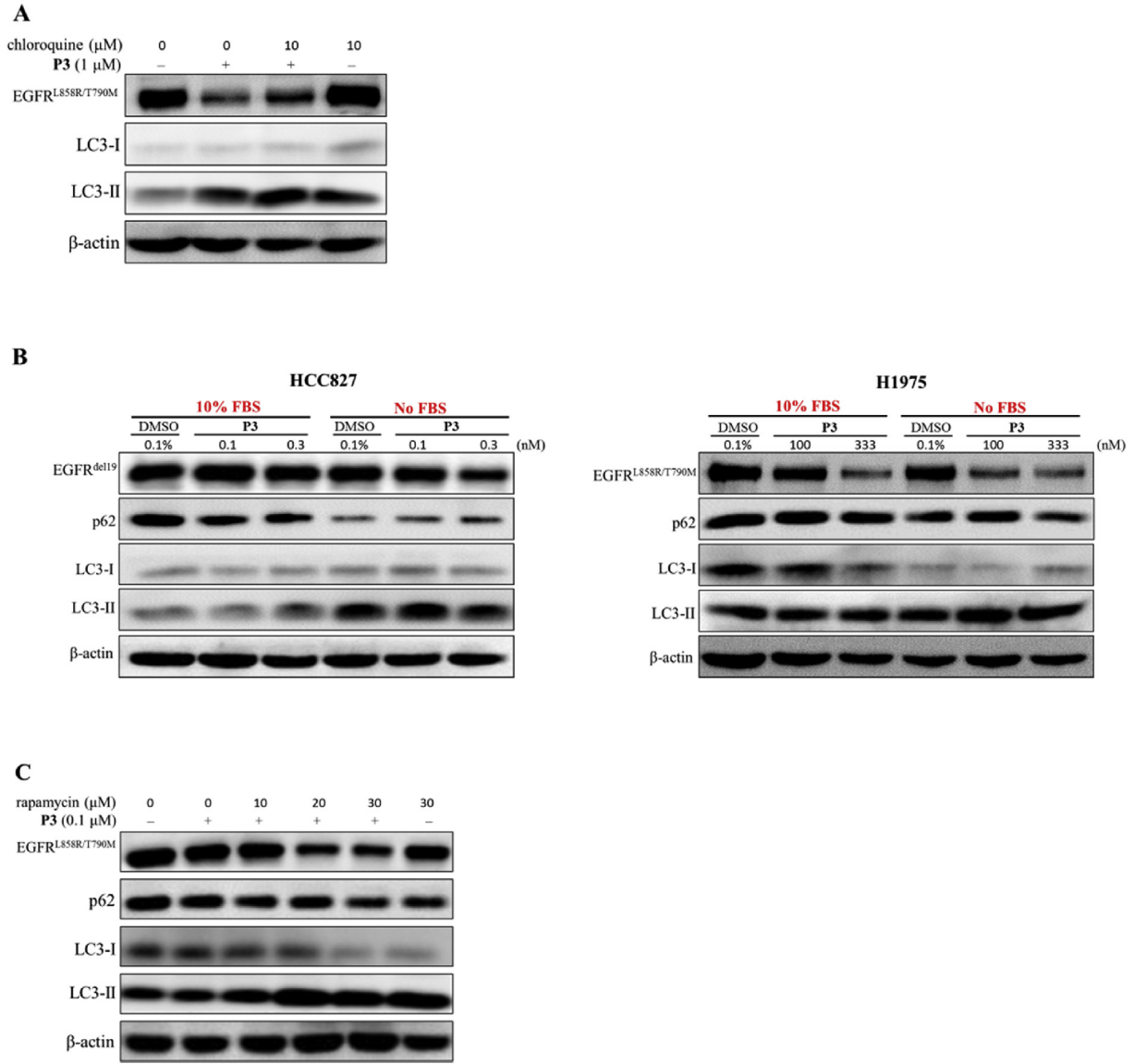


Fig. 9. Exploring relationship between EGFR degradation and autophagy. (A) H1975 cell line was pretreated with chloroquine for 2 h followed by 24 h treatment with P3. (B) HCC827 or H1975 cell lines were pre-cultured using medium with or without FBS for 8 h followed by 16 h treatment with P3 under indicated concentrations. (C) H1975 cell line was pretreated with rapamycin under indicated concentrations for 8 h followed by 16 h treatment with P3. Protein level was analyzed by Western blotting (n = 3).

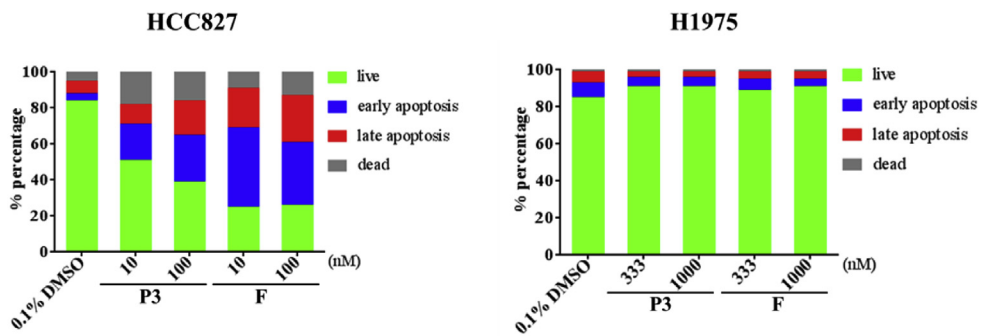


Fig. 10. Flow cytometry analysis of cell apoptosis induced by P3 and its parental compound F. Cell lines were treated with indicated concentration for 48 h (n = 2).

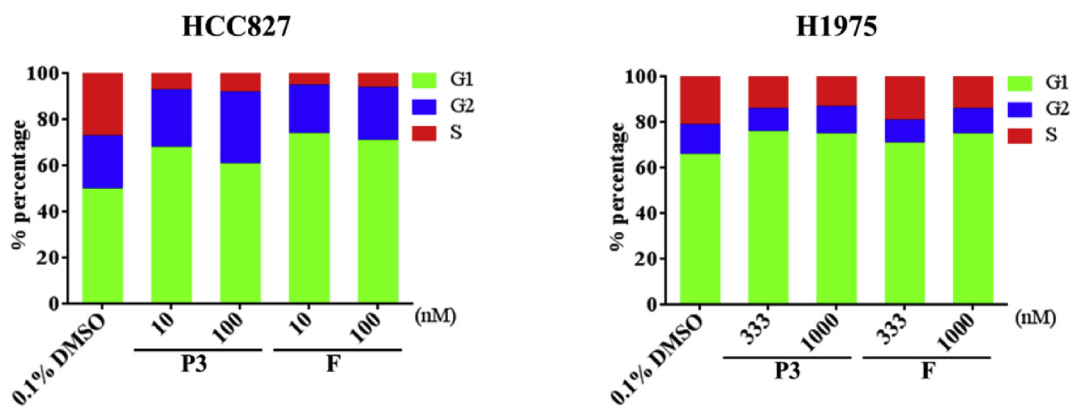


Fig. 11. The effect of P3 and its parental compound F on cell cycle analyzed by flow cytometry. Cell lines were treated with indicated concentrations for 48 h (n = 2).

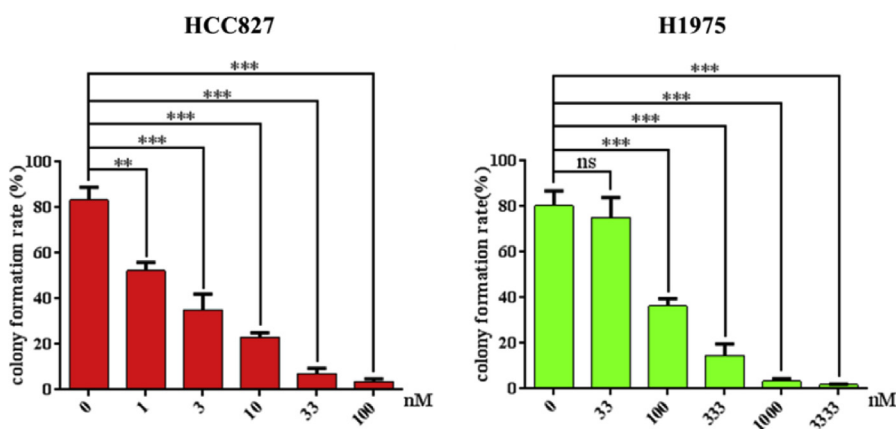


Fig. 12. Colony formation assay. Cell were seeded on 6-well plate and treated with P3 under indicated concentrations for 15 days. And the cells were stained with crystal violet. Colony number was counted (n = 3, *P < 0.05, **P < 0.01, ***P < 0.001).

compound **4** without further purification. Gray solid, 94% yield, ^1H NMR (400 MHz, CDCl_3) δ 7.54 (s, 1H), 7.51 (d, $J = 8.9$ Hz, 2H), 6.89 (d, $J = 8.9$ Hz, 2H), 6.77 (s, 1H), 5.20 (d, $J = 6.8$ Hz, 1H), 4.44–4.26 (m, 1H), 3.69–3.53 (m, 4H), 3.13–2.98 (m, 4H), 2.16–2.05 (m, 2H), 1.80–1.62 (m, 4H), 1.55–1.50 (m, 2H), 1.48 (s, 9H). MS (ESI): m/z calcd for $\text{C}_{24}\text{H}_{36}\text{N}_7\text{O}_2$: 454.3 $[\text{M}+\text{H}]^+$; found: 454.5.

4.1.4. Tert-butyl 4-(4-((9-cyclopentyl-8-(phenylamino)-9H-purin-2-yl)amino)phenyl)pi perazine-1-carboxylate (**5**)

To a round bottom flask were added **4** (4.00 g, 8.82 mmol), EDCI (2.03 g, 10.58 mmol), 1,2-dichloroethane (50 mL), phenyl isothiocyanate (1.43 g, 10.58 mmol) and DIPEA (1.37 g, 10.58 mmol). The resulted mixture was stirred at 65 °C for 5 h. Product **5** was isolated using column chromatography (DCM:MeOH = 50:1). Pale yellow solid, 92% yield, ^1H NMR (400 MHz, CDCl_3) δ 8.41 (s, 1H), 7.54 (dd, $J = 7.6, 5.3$ Hz, 4H), 7.38 (t, $J = 8.0$ Hz, 2H), 7.22 (s, 1H), 7.09 (t, $J = 7.4$ Hz, 1H), 6.94 (d, $J = 8.9$ Hz, 2H), 6.33 (s, 1H), 4.75–4.59 (m, 1H), 3.69–3.53 (m, 4H), 3.20–3.01 (m, 4H), 2.52–2.37 (m, 2H), 2.19–2.01 (m, 4H), 1.83–1.72 (m, 2H), 1.49 (s, 9H). MS (ESI): m/z calcd for $\text{C}_{31}\text{H}_{39}\text{N}_8\text{O}_2$: 555.3 $[\text{M}+\text{H}]^+$; found: 555.6.

4.1.5. 9-Cyclopentyl-8-phenylamino-2-(4-(piperazin-1-yl)phenylamino)-9H-purine (**6**)

To a solution of **5** (2.86 g, 5.16 mmol) in DCM (15 mL) were added TFA (10 mL), and the solution was stirred at room temperature overnight. The solvent was evaporated under vacuum.

Subsequently, the pH of the residue was adjusted to 10 using saturated aqueous Na_2CO_3 . The precipitate was filtered to obtain intermediate **6**. Yellow solid, 90% yield, ^1H NMR (400 MHz, $\text{DMSO}-d_6$) δ 9.03 (d, $J = 4.7$ Hz, 2H), 8.36 (s, 1H), 7.81 (d, $J = 8.0$ Hz, 2H), 7.65 (d, $J = 8.9$ Hz, 2H), 7.33 (t, $J = 7.9$ Hz, 2H), 6.98 (t, $J = 7.3$ Hz, 1H), 6.90 (d, $J = 9.0$ Hz, 2H), 5.01–4.90 (m, 1H), 3.13 (s, 4H), 3.11 (s, 4H), 2.05 (s, 5H), 1.69 (d, $J = 5.1$ Hz, 3H). MS (ESI): m/z calcd for $\text{C}_{26}\text{H}_{31}\text{N}_8$: 455.3 $[\text{M}+\text{H}]^+$; found: 455.5.

4.1.6. Ethyl 7-(4-(4-((9-cyclopentyl-8-(phenylamino)-9H-purin-2-yl)amino)phenyl)pi-perazin-1-yl)heptanoate (**7**)

To a flask were added **6** (0.30 g, 0.66 mmol), ethyl 7-bromoheptanoate (0.30 g, 1.32 mmol), K_2CO_3 (0.18 g, 1.32 mmol), NaI (0.04 g, 0.26 mmol) and CH_3CN . The resulted mixture was heated at reflux for 3 h. The solvent was evaporated under reduced pressure, and the residue was purified using column chromatography (DCM: MeOH = 30:1) to produce **7**. Pale yellow solid, 50% yield, ^1H NMR (400 MHz, CDCl_3) δ 8.45 (s, 1H), 7.53 (t, $J = 8.2$ Hz, 4H), 7.37 (t, $J = 7.9$ Hz, 2H), 7.08 (t, $J = 7.4$ Hz, 1H), 6.93 (d, $J = 9.0$ Hz, 3H), 6.35 (s, 1H), 4.73–4.60 (m, 1H), 4.13 (q, $J = 7.1$ Hz, 2H), 3.20 (s, 4H), 2.68 (s, 4H), 2.51–2.38 (m, 4H), 2.30 (t, $J = 7.5$ Hz, 2H), 2.18–2.01 (m, 4H), 1.82–1.71 (m, 2H), 1.68–1.61 (m, 2H), 1.61–1.53 (m, 2H), 1.40–1.32 (m, 4H), 1.26 (t, $J = 7.1$ Hz, 3H). MS (ESI): m/z calcd for $\text{C}_{35}\text{H}_{47}\text{N}_8\text{O}_2$: 611.4 $[\text{M}+\text{H}]^+$; found: 611.5.

4.1.7. 7-(4-(4-((9-cyclopentyl-8-(phenylamino)-9H-purin-2-yl)amino)phenyl)pipe-razin-1-yl)heptanoic acid (**8**)

To a flask were added **7** (0.20 g, 0.33 mmol), NaOH (0.26 g, 6.6 mmol), H₂O (2 mL) and EtOH (4 mL). The resulted suspension was stirred at room temperature for 6 h. The solvent was evaporated under reduced pressure, and the pH of the residue was adjusted to 5 using 1 M HCl. The precipitate was filtered to obtain compound **8**. Yellow solid, 79% yield, ¹H NMR (400 MHz, DMSO-*d*₆) δ 12.02 (s, 1H), 10.35 (s, 1H), 9.13 (s, 1H), 8.36 (s, 1H), 7.83 (d, *J* = 7.8 Hz, 2H), 7.66 (d, *J* = 8.9 Hz, 2H), 7.33 (t, *J* = 7.9 Hz, 2H), 6.99 (t, *J* = 7.4 Hz, 1H), 6.95 (d, *J* = 8.8 Hz, 2H), 5.08–4.94 (m, 1H), 3.69 (d, *J* = 11.7 Hz, 2H), 3.55 (d, *J* = 11.1 Hz, 2H), 3.15–2.99 (m, 6H), 2.23 (t, *J* = 7.3 Hz, 2H), 2.04 (s, 5H), 1.70 (s, 5H), 1.55–1.48 (m, 2H), 1.32 (s, 4H). MS (ESI): *m/z* calcd for C₃₃H₄₃N₈O₂: 583.4 [M+H]⁺; found: 583.6.

4.1.8. 8-Bromo-N-(2-(2,6-dioxopiperidin-3-yl)-1-oxoisindolin-4-yl)octanamide (**9a**)

Lenalidomide (0.50 g, 1.93 mmol), 8-bromooctanoic acid (0.50 g, 2.31 mmol), EDCI (0.44 g, 2.31 mmol), DMAP (0.28, 2.31 mmol) and DMF (10 mL) were mixed in a flask. The suspension was stirred in an oil bath at 40 °C for 4 h. The solvent was evaporated under vacuum. The residue was isolated using column chromatography (DCM:MeOH = 50:1) to give compound **9a**. White solid, 35% yield, ¹H NMR (400 MHz, DMSO-*d*₆) δ 11.03 (s, 1H), 9.77 (s, 1H), 7.81 (dd, *J* = 7.0, 1.7 Hz, 1H), 7.54–7.46 (m, 2H), 5.15 (dd, *J* = 13.3, 5.0 Hz, 1H), 4.36 (q, *J* = 17.5 Hz, 2H), 3.63 (t, *J* = 6.6 Hz, 2H), 3.00–2.84 (m, 1H), 2.61 (d, *J* = 16.8 Hz, 1H), 2.41–2.31 (m, 3H), 2.09–1.99 (m, 1H), 1.76–1.66 (m, 2H), 1.66–1.56 (m, 2H), 1.47–1.24 (m, 6H).

4.1.9. (2*S*,4*R*)-1-((*S*)-2-(8-bromooctanamido)-3,3-dimethylbutanoyl)-4-hydroxy-N-(4-(4-methylthiazol-5-yl)benzyl)pyrrolidine-2-carboxamide (**9b**)

To a solution of 8-bromooctanoic acid (0.12 g, 0.56 mmol) and **VHL-L** (0.20 g, 0.46 mmol) in DCM (3 mL) were added HATU (0.21 g, 0.56 mmol) and DIPEA (0.12 g, 0.92 mmol). The mixture was stirred at room temperature for 3.5 h. The reaction mixture was diluted with DCM (80 mL) and washed with water (3 × 20 mL). The organic phase was washed with saturated brine (20 mL), dried with anhydrous sodium sulfate and isolated using column chromatography to give compound **9b**. White solid, 83% yield, ¹H NMR (400 MHz, DMSO-*d*₆) δ 9.00 (s, 1H), 8.58 (t, *J* = 6.0 Hz, 1H), 7.86 (d, *J* = 9.2 Hz, 1H), 7.56–7.46 (m, 2H), 7.40 (q, *J* = 8.3 Hz, 2H), 4.55 (d, *J* = 9.3 Hz, 2H), 4.48–4.40 (m, 3H), 4.35 (s, 1H), 4.22 (dd, *J* = 15.9, 5.4 Hz, 1H), 3.69–3.63 (m, 1H), 3.52 (t, *J* = 6.7 Hz, 2H), 2.52–2.49 (m, 4H), 2.45 (s, 3H), 1.94–1.84 (m, 2H), 1.82–1.73 (m, 2H), 1.36 (s, 6H), 0.94 (s, 9H). MS (ESI): *m/z* calcd for C₃₀H₄₃BrN₄NaO₄S: 657.2 [M+Na]⁺; found: 657.4 (⁷⁹Br), 659.4 (⁸¹Br).

4.1.10. Tert-butyl 2-methylaminoacetate (**10**)

To a solution of methylamine (0.80 g, 25.6 mmol) in CH₃CN (3 mL) were added NaI (0.15 g, 1.02 mmol), and the suspension was stirred in an ice bath for 5 min. Subsequently, *tert*-butyl 2-bromoacetate (0.50 g, 2.56 mmol) in CH₃CN (7 mL) was added dropwise. The resulted mixture was stirred at room temperature overnight. The solvent was evaporated under vacuum, and the water was added (10 mL). The water phase was extracted with ethyl acetate (4 × 20 mL), and the combined organic phase was washed with saturated brine and dried with anhydrous sodium sulfate. Compound **10** was obtained by filtration followed by evaporating the solvent without further purification. Yellow oil, 46% yield, ¹H NMR (400 MHz, CDCl₃) δ 3.26 (s, 2H), 2.43 (s, 3H), 1.76 (s, 1H), 1.47 (s, 9H). MS (ESI): *m/z* calcd for C₇H₁₆NO₂: 146.1 [M+H]⁺; found: 146.4.

4.1.11. 2-(2-(2-(4-(4-((9-cyclopentyl-8-(phenylamino)-9H-purin-2-yl)amino)phen-yl)piperazin-1-yl)ethoxy)ethoxy)ethyl 4-methylbenzenesulfonate (**11a**)

A flask was charged with **6** (0.40 g, 0.88 mmol), tri (ethyl-ene glycol) di-*p*-toluenesulfonate (0.82 g, 1.76 mmol), K₂CO₃ (0.25 g, 1.76 mmol), KI (0.03 g, 0.18 mmol) and CH₃CN (5 mL). The resulted suspension was heated at 65 °C overnight. The reaction mixture was isolated using column chromatography (DCM:MeOH = 50:1–30:1) to produce compound **11a**. Yellow solid, 26% yield, ¹H NMR (400 MHz, CDCl₃) δ 8.45 (s, 1H), 7.80 (d, *J* = 8.2 Hz, 2H), 7.58–7.49 (m, 4H), 7.40–7.31 (m, 4H), 7.07 (t, *J* = 7.3 Hz, 1H), 6.99–6.89 (m, 3H), 6.38 (s, 1H), 4.74–4.60 (m, 1H), 4.20–4.12 (m, 2H), 3.72–3.68 (m, 2H), 3.66 (t, *J* = 5.7 Hz, 2H), 3.62–3.55 (m, 4H), 3.21–3.13 (m, 4H), 2.77–2.65 (m, 6H), 2.44 (s, 3H), 2.16–2.00 (m, 5H), 1.80–1.69 (m, 3H). MS (ESI): *m/z* calcd for C₃₉H₄₉N₈O₅S: 741.4 [M+H]⁺; found: 741.5.

4.1.12. 2-(2-(2-(2-(4-(4-((9-cyclopentyl-8-(phenylamino)-9H-purin-2-yl)amino)ph-en-yl)piperazin-1-yl)ethoxy)ethoxy)ethoxy)ethyl 4-methylbenzenesulfonate (**11b**)

Compound **11b** was prepared similarly as described for **11a**. Yellow oil, 22% yield, ¹H NMR (400 MHz, CDCl₃) δ 8.44 (s, 1H), 7.80 (d, *J* = 8.3 Hz, 2H), 7.62–7.48 (m, 4H), 7.42–7.31 (m, 4H), 7.07 (t, *J* = 7.4 Hz, 1H), 6.99–6.88 (m, 3H), 6.45 (s, 1H), 4.72–4.61 (m, 1H), 4.16 (t, *J* = 4.1 Hz, 2H), 3.71–3.65 (m, 6H), 3.63 (s, 4H), 3.60 (s, 2H), 3.23–3.10 (m, 4H), 2.78–2.61 (m, 6H), 2.44 (s, 3H), 2.17–1.99 (m, 5H), 1.88 (s, 3H). MS (ESI): *m/z* calcd for C₄₁H₅₃N₈O₆S: 785.4 [M+H]⁺; found: 785.5.

4.1.13. 2-(2-(2-(2-(2-(4-(4-((9-cyclopentyl-8-(phenylamino)-9H-purin-2-yl)amino)-phenyl)piperazin-1-yl)ethoxy)ethoxy)ethoxy)ethyl 4-methylbenzenesulfonate (**11c**)

Compound **11c** was prepared similarly as described for **11a**. Yellow oil, 36% yield, ¹H NMR (400 MHz, DMSO-*d*₆) δ 9.10–8.94 (m, 2H), 8.36 (s, 1H), 7.87–7.76 (m, 3H), 7.69 (d, *J* = 8.9 Hz, 1H), 7.61 (d, *J* = 8.9 Hz, 1H), 7.48 (dd, *J* = 8.0, 4.4 Hz, 2H), 7.33 (t, *J* = 7.9 Hz, 2H), 7.11 (d, *J* = 7.8 Hz, 1H), 6.98 (t, *J* = 7.3 Hz, 2H), 6.86 (d, *J* = 8.9 Hz, 1H), 5.03–4.84 (m, 1H), 4.59 (t, *J* = 5.5 Hz, 2H), 3.58–3.55 (m, 4H), 3.52–3.50 (m, 12H), 3.48 (s, 2H), 3.45 (s, 2H), 3.42 (d, *J* = 5.0 Hz, 4H), 3.03 (s, 2H), 2.51 (s, 3H), 2.41 (s, 1H), 2.28 (s, 1H), 2.04 (s, 4H), 1.69 (s, 2H). MS (ESI): *m/z* calcd for C₄₃H₅₇N₈O₇S: 829.4 [M+H]⁺; found: 829.6.

4.1.14. Tert-butyl 2-((N-(2-(2-(2-(4-(4-((9-cyclopentyl-8-(phenylamino)-9H-purin-2-yl)amino)phenyl)piperazin-1-yl)ethoxy)ethoxy)ethyl)-N-methylamino)acetate (**12a**)

11a (0.15 g, 0.20 mmol), **10** (0.0637 g, 0.40 mmol), K₂CO₃ (0.0552 g, 0.40 mmol) and NaI (0.0120 g, 0.08 mmol) were suspended in CH₃CN (3 mL). The resulted mixture was heated at reflux under argon atmosphere for 11 h. The solvent was evaporated under vacuum and the residue was isolated using column chromatography (DCM:MeOH = 30:1–15:1) to give product **12a**. Yellow solid, 64% yield, ¹H NMR (400 MHz, DMSO-*d*₆) δ 8.99 (d, *J* = 7.2 Hz, 2H), 8.35 (s, 1H), 7.81 (d, *J* = 7.8 Hz, 2H), 7.61 (d, *J* = 9.0 Hz, 2H), 7.33 (t, *J* = 7.9 Hz, 2H), 6.98 (t, *J* = 7.3 Hz, 1H), 6.86 (d, *J* = 9.0 Hz, 2H), 5.02–4.89 (m, 1H), 3.56 (t, *J* = 5.7 Hz, 2H), 3.53–3.46 (m, 6H), 3.19 (s, 2H), 3.05 (s, 4H), 2.65 (t, *J* = 5.9 Hz, 4H), 2.61 (s, 4H), 2.31 (s, 3H), 2.04 (s, 5H), 1.81–1.61 (m, 3H), 1.41 (s, 9H). MS (ESI): *m/z* calcd for C₃₉H₅₆N₉O₄: 714.4 [M+H]⁺; found: 714.6.

4.1.15. Tert-butyl 2-((N-(2-(2-(2-(2-(4-(4-((9-cyclopentyl-8-(phenylamino)-9H-purin-2-yl)amino)phenyl)piperazin-1-yl)ethoxy)ethoxy)ethyl)-N-methylamino)acetate (**12b**)

Compound **12b** was prepared similarly as described for **12a**. Yellow oil, 68% yield, ¹H NMR (400 MHz, DMSO-*d*₆) δ 9.01 (s, 2H),

8.35 (s, 1H), 7.81 (d, $J = 7.8$ Hz, 2H), 7.62 (d, $J = 8.9$ Hz, 2H), 7.33 (t, $J = 7.9$ Hz, 2H), 6.98 (t, $J = 7.3$ Hz, 1H), 6.88 (d, $J = 8.9$ Hz, 2H), 5.02–4.87 (m, 1H), 3.61 (s, 2H), 3.56–3.46 (m, 10H), 3.20 (s, 2H), 3.11 (s, 4H), 2.70–2.62 (m, 4H), 2.54 (s, 4H), 2.31 (s, 3H), 2.04 (s, 5H), 1.70 (s, 3H), 1.40 (s, 9H). MS (ESI): m/z calcd for $C_{41}H_{60}N_9O_5$: 758.5 $[M+H]^+$; found: 758.6.

4.1.16. Tert-butyl 2-((N-(2-(2-(2-(2-(2-(4-(4-((9-cyclopentyl-8-(phenylamino)-9H-purin-2-yl)amino)phenyl)piperazin-1-yl)ethoxy)ethoxy)ethoxy)ethyl)-N-methyl)amino)acetate (12c**)**

Compound **12c** was prepared similarly as described for **12a**. Yellow solid, 36% yield, 1H NMR (400 MHz, DMSO- d_6) δ 9.02 (d, $J = 3.0$ Hz, 2H), 8.35 (s, 1H), 7.81 (d, $J = 8.0$ Hz, 2H), 7.64 (d, $J = 8.9$ Hz, 2H), 7.33 (t, $J = 7.9$ Hz, 2H), 6.98 (t, $J = 7.3$ Hz, 1H), 6.90 (d, $J = 8.9$ Hz, 2H), 5.01–4.88 (m, 1H), 3.64–3.44 (m, 16H), 3.23 (s, 2H), 3.17 (s, 4H), 2.94 (s, 4H), 2.72–2.63 (m, 4H), 2.33 (s, 3H), 2.04 (s, 5H), 1.70 (s, 3H), 1.40 (s, 9H). MS (ESI): m/z calcd for $C_{43}H_{64}N_9O_6$: 802.5 $[M+H]^+$; found: 802.7.

4.1.17. (2S,4R)-1-((S)-2-acetamido-3,3-dimethylbutanoyl)-4-hydroxy-N-(4-(4-methyl-thiazol-5-yl)benzyl)pyrrolidine-2-carboxamide (VHL-Ac)

To a solution of **VHL-L** (0.12 g, 0.25 mmol) in DCM (2 mL) were added acetic anhydride (0.04 g, 0.38 mmol). The resulted solution was stirred at room temperature for 1 h. Compound **VHL-Ac** was isolated using column chromatography (DCM:MeOH = 50:1–30:1). White solid, 56% yield, 1H NMR (400 MHz, DMSO- d_6) δ 8.99 (s, 1H), 8.58 (t, $J = 6.0$ Hz, 1H), 7.96 (d, $J = 9.4$ Hz, 1H), 7.40 (q, $J = 8.4$ Hz, 4H), 5.13 (d, $J = 3.5$ Hz, 1H), 4.54 (d, $J = 9.5$ Hz, 1H), 4.47–4.40 (m, 2H), 4.35 (s, 1H), 4.21 (dd, $J = 15.9, 5.4$ Hz, 1H), 3.70–3.62 (m, 2H), 2.44 (s, 3H), 2.07–1.98 (m, 1H), 1.89 (s, 3H), 0.94 (s, 9H). MS (ESI): m/z calcd for $C_{24}H_{22}N_4O_4S$: 473.2 $[M+H]^+$; found: 473.4.

4.1.18. 7-(4-(4-((9-cyclopentyl-8-(phenylamino)-9H-purin-2-yl)amino)phenyl)piperazin-1-yl)-N-(2-(2,6-dioxopiperidin-3-yl)-1-oxoisindolin-4-yl)heptanamide (P1)

A flask was charged with **8** (0.0701 g, 0.12 mmol), lenalidomide (0.0467 g, 0.18 mmol), HATU (0.0684 g, 0.18 mmol), DIPEA (0.0310 g, 0.24 mmol) and DMF (1 mL). The resulted mixture was stirred at room temperature overnight. The solvent was evaporated under vacuum, and the residue was isolated using column chromatography (DCM:MeOH = 20:1–8:1) to give target compound **P1** which was subsequently washed with ethyl acetate to obtain pure product. Yellow solid, 51% yield, 1H NMR (400 MHz, DMSO- d_6) δ 11.05 (s, 1H), 9.92 (s, 1H), 9.14 (s, 1H), 9.07 (s, 1H), 8.37 (s, 1H), 7.85 (d, $J = 8.0$ Hz, 3H), 7.67 (d, $J = 8.7$ Hz, 2H), 7.52 (t, $J = 7.5$ Hz, 2H), 7.33 (t, $J = 7.8$ Hz, 2H), 6.99 (t, $J = 7.3$ Hz, 1H), 6.93 (d, $J = 8.8$ Hz, 2H), 5.17 (dd, $J = 13.2, 4.9$ Hz, 1H), 5.09–4.96 (m, 1H), 4.40 (q, $J = 17.5$ Hz, 2H), 3.19 (d, $J = 10.6$ Hz, 4H), 3.11–2.84 (m, 5H), 2.69–2.56 (m, 2H), 2.46 (s, 2H), 2.43–2.33 (m, 3H), 2.05 (s, 5H), 1.78–1.60 (m, 7H), 1.36 (s, 4H). ^{13}C NMR (100 MHz, DMSO- d_6) δ 173.4, 171.8, 171.6, 168.3, 154.7, 152.9, 149.7, 144.5, 143.2, 140.9, 135.2, 134.3, 134.2, 133.1, 129.1 (2C), 127.5, 125.8, 122.0, 119.6 (2C), 119.5, 190.0 (2C), 117.0 (2C), 56.3, 54.9, 52.0, 51.6 (2C), 47.4 (2C), 47.1, 36.1, 31.7, 29.5 (2C), 28.7 (2C), 26.5, 25.3, 24.9 (2C), 24.0, 23.1. HRMS (ESI): m/z calcd for $C_{46}H_{54}N_{11}O_4$: 824.43602 $[M+H]^+$; found: 824.43462.

4.1.19. 8-(4-(4-((9-cyclopentyl-8-(phenylamino)-9H-purin-2-yl)amino)phenyl)piperazin-1-yl)-N-(2-(2,6-dioxopiperidin-3-yl)-1-oxoisindolin-4-yl)octanamide (P2)

To a flask were added **6** (0.10 g, 0.22 mmol), **9a** (0.15 g, 0.33 mmol), DIPEA (0.0568 g, 0.44 mmol), KI (0.0073 g, 0.044 mmol) and NMP (2 mL). The suspension was heated at 100 °C in an oil bath overnight. The reaction mixture was diluted with DCM (80 mL) and washed with water (5 × 20 mL) and saturated

brine (20 mL). The organic phase was dried with anhydrous sodium sulfate and isolated using column chromatography (DCM:MeOH = 30:1–50:1) followed by wash with ethyl acetate to give compound **P2**. Yellow solid, 26% yield, 1H NMR (400 MHz, DMSO- d_6) δ 11.06 (s, 1H), 9.83 (s, 1H), 9.07 (s, 1H), 9.00 (s, 1H), 8.36 (s, 1H), 7.84 (d, $J = 7.7$ Hz, 3H), 7.63 (d, $J = 8.9$ Hz, 2H), 7.56–7.45 (m, 2H), 7.33 (t, $J = 7.9$ Hz, 2H), 6.98 (t, $J = 7.3$ Hz, 1H), 6.88 (d, $J = 9.0$ Hz, 2H), 5.16 (dd, $J = 13.3, 5.1$ Hz, 1H), 5.05–4.92 (m, 1H), 4.38 (q, $J = 17.5$ Hz, 2H), 3.12 (s, 4H), 2.98–2.88 (m, 1H), 2.70 (s, 4H), 2.65–2.58 (m, 2H), 2.47 (s, 2H), 2.40–2.30 (m, 3H), 2.05 (s, 5H), 1.76–1.58 (m, 5H), 1.52 (s, 2H), 1.33 (s, 6H). ^{13}C NMR (100 MHz, DMSO- d_6) δ 173.3, 171.9, 171.6, 168.3, 154.8, 152.9, 149.6, 145.5, 143.3, 140.9, 134.6, 134.3, 134.2, 133.1, 129.1 (2C), 127.4, 125.7, 122.0, 119.6 (2C), 119.4, 118.9 (2C), 116.6 (2C), 57.8, 55.4, 54.8, 52.8, 52.0 (2C), 49.0, 47.0 (2C), 36.3, 31.7, 29.5 (2C), 29.1 (2C), 27.1, 25.5, 24.9 (2C), 23.1, 21.5. HRMS (ESI): m/z calcd for $C_{47}H_{56}N_{11}O_4$: 838.45167 $[M+H]^+$; found: 838.45145.

4.1.20. (2S,4R)-1-((S)-2-(7-(4-(4-((9-cyclopentyl-8-(phenylamino)-9H-purin-2-yl)amino)phenyl)piperazin-1-yl)heptanamido)-3,3-dimethylbutanoyl)-4-hydroxy-N-(4-(4-methylthiazol-5-yl)benzyl)pyrrolidine-2-carboxamide (P3)

Compound **P3** was prepared similarly as described for **P1** using **VHL-L** as E3-recruitment element. Yellow solid, 51% yield, 1H NMR (400 MHz, DMSO- d_6) δ 9.14 (s, 1H), 9.05 (s, 1H), 8.99 (s, 1H), 8.61 (t, $J = 5.7$ Hz, 1H), 8.37 (s, 1H), 7.93–7.81 (m, 3H), 7.66 (d, $J = 8.7$ Hz, 2H), 7.46–7.37 (m, 4H), 7.33 (t, $J = 7.7$ Hz, 2H), 6.98 (t, $J = 7.3$ Hz, 1H), 6.92 (d, $J = 8.7$ Hz, 2H), 5.19 (s, 1H), 5.08–4.95 (m, 1H), 4.57 (d, $J = 9.3$ Hz, 1H), 4.49–4.41 (m, 2H), 4.37 (s, 1H), 4.23 (dd, $J = 15.8, 5.1$ Hz, 1H), 3.67 (s, 2H), 3.27 (s, 4H), 3.08 (s, 4H), 2.85 (s, 2H), 2.45 (s, 5H), 2.34–2.24 (m, 1H), 2.22–2.12 (m, 1H), 2.05 (s, 5H), 1.96–1.87 (m, 1H), 1.75–1.60 (m, 4H), 1.56–1.46 (m, 2H), 1.38–1.20 (m, 4H), 0.96 (s, 9H). ^{13}C NMR (100 MHz, DMSO- d_6) δ 172.5, 172.4, 170.2, 154.8, 152.9, 151.9, 149.7, 148.2, 144.8, 143.3, 140.9, 140.0, 135.1, 131.6, 130.1, 129.1 (2C), 129.1 (2C), 127.9 (2C), 127.5, 122.0, 119.6 (2C), 119.0 (2C), 116.9 (2C), 69.4, 59.2, 56.8, 56.8 (2C), 54.8, 51.9 (2C), 47.8, 42.1, 38.5, 35.7 (2C), 35.2, 29.5 (2C), 28.7 (2C), 26.9 (3C), 26.6, 25.7, 24.9 (2C), 16.41. HRMS (ESI): m/z calcd for $C_{55}H_{71}N_{12}O_4S$: 995.54419 $[M+H]^+$; found: 995.54146.

4.1.21. (2S,4R)-1-((S)-2-(8-(4-(4-((9-cyclopentyl-8-(phenylamino)-9H-purin-2-yl)amino)phenyl)piperazin-1-yl)octanamido)-3,3-dimethylbutanoyl)-4-hydroxy-N-(4-(4-methylthiazol-5-yl)benzyl)pyrrolidine-2-carboxamide (P4)

A flask was charged with **6** (0.09 g, 0.19 mmol), **9b** (0.12 g, 0.19 mmol), K_2CO_3 (0.05 g, 0.38 mmol), KI (0.0063 g, 0.04 mmol) and CH_3CN (3 mL). The mixture was heated at 80 °C in an oil bath overnight. The solvent was evaporated under vacuum, and the residue was purified using column chromatography (DCM:MeOH = 30:1–10:1) followed by wash with ethyl acetate to produce **P4**. Yellow solid, 63% yield, 1H NMR (400 MHz, DMSO- d_6) δ 9.03 (d, $J = 7.6$ Hz, 2H), 8.98 (s, 1H), 8.59 (t, $J = 5.9$ Hz, 1H), 8.36 (s, 1H), 7.88 (d, $J = 9.4$ Hz, 1H), 7.83 (d, $J = 7.9$ Hz, 2H), 7.64 (d, $J = 8.8$ Hz, 2H), 7.45–7.37 (m, 4H), 7.33 (t, $J = 7.9$ Hz, 2H), 6.99 (t, $J = 7.3$ Hz, 1H), 6.89 (d, $J = 8.8$ Hz, 2H), 5.16 (s, 1H), 5.03–4.91 (m, 1H), 4.57 (d, $J = 9.4$ Hz, 1H), 4.49–4.41 (m, 2H), 4.37 (s, 1H), 4.23 (dd, $J = 15.8, 5.3$ Hz, 1H), 3.72–3.63 (m, 2H), 3.37–3.30 (m, 2H), 3.12 (s, 4H), 2.71 (s, 4H), 2.45 (s, 5H), 2.33–2.24 (m, 1H), 2.18–2.11 (m, 1H), 2.05 (s, 5H), 1.95–1.88 (m, 1H), 1.70 (s, 2H), 1.56–1.44 (m, 4H), 1.28 (s, 6H), 0.95 (s, 9H). ^{13}C NMR (100 MHz, DMSO- d_6) δ 172.6, 172.4, 170.2, 154.8, 152.9, 151.9, 149.6, 148.2, 145.4, 143.3, 140.9, 140.0, 134.6, 131.6, 130.1, 129.1 (2C), 129.1 (2C), 127.9 (2C), 127.4, 122.0, 119.6 (2C), 118.9 (2C), 116.6 (2C), 69.3, 59.2, 56.8, 56.8 (2C), 54.8, 52.8 (2C), 49.0, 42.1, 38.4, 35.7 (2C), 35.3, 29.5 (2C), 29.1 (2C), 27.1, 26.9, 26.9 (3C), 25.8, 24.9 (2C), 16.4. HRMS (ESI): m/z calcd for

C₅₆H₇₃N₁₂O₄S: 1009.55984 [M+H]⁺; found: 1009.55876.

4.1.22. 2-((2-(2-(2-(4-(4-((9-cyclopentyl-8-(phenylamino)-9H-purin-2-yl)amino)phen-yl)piperazin-1-yl)ethoxy)ethoxy)ethyl)(methyl)amino)-N-(2-(2,6-dioxopiperidin-3-yl)-1-oxoisindolin-4-yl)acetamide (**P5**)

To a solution of **12a** (0.08 g, 0.11 mmol) in DCM (1 mL) were added TFA (1 mL). The resulted solution was stirred at room temperature for 8 h. The solvent was evaporated under high vacuum. To the residue was added DMF (1 mL), DIPEA (0.28 g, 2.2 mmol), HATU (0.08 g, 0.22 mmol) and lenalidomide (0.0570 g, 0.22 mmol). The mixture was stirred at room temperature for 4 h. To the reaction mixture was added DCM (100 mL), and the solution was washed with water (3 × 20 mL) and saturated brine (20 mL) and dried with anhydrous sodium sulfate. Compound **P5** was obtained using column chromatography (DCM:MeOH = 20:1–16:1) followed by wash using PE:EA (5:1). Yellow solid, 31% yield, ¹H NMR (400 MHz, DMSO-*d*₆) δ 11.05 (s, 1H), 9.72 (s, 1H), 9.00 (d, *J* = 10.5 Hz, 2H), 8.36 (s, 1H), 7.92–7.76 (m, 3H), 7.61 (d, *J* = 8.6 Hz, 2H), 7.57–7.48 (m, 2H), 7.33 (t, *J* = 7.6 Hz, 2H), 6.98 (t, *J* = 7.2 Hz, 1H), 6.85 (d, *J* = 8.7 Hz, 2H), 5.16 (dd, *J* = 13.0, 4.7 Hz, 1H), 5.04–4.89 (m, 1H), 4.39 (q, *J* = 17.3 Hz, 2H), 3.63–3.56 (m, 2H), 3.53 (s, 2H), 3.46 (d, *J* = 5.6 Hz, 4H), 3.25 (s, 2H), 3.00 (s, 4H), 2.94–2.85 (m, 1H), 2.68 (s, 2H), 2.65–2.56 (m, 1H), 2.51 (s, 4H), 2.46–2.36 (m, 7H), 2.04 (s, 6H), 1.69 (s, 2H). ¹³C NMR (100 MHz, DMSO-*d*₆) δ 173.3, 171.5, 169.7, 168.3, 154.9, 152.9, 149.6, 145.9, 143.3, 140.9, 134.5, 134.3, 133.7, 133.2, 129.2, 129.1 (2C), 127.4, 125.8, 122.0, 119.8, 119.7 (2C), 118.9 (2C), 116.4 (2C), 70.1, 70.0, 68.8, 68.8, 61.5, 57.6, 56.9, 54.8 (2C), 53.6, 52.0 (2C), 49.7, 46.7, 43.5, 31.7, 29.5 (2C), 24.9 (2C), 23.0. HRMS (ESI): *m/z* calcd for C₄₈H₅₉N₁₂O₆: 899.46805 [M+H]⁺; found: 899.46376.

4.1.23. 2-(2-(2-(2-(2-(4-(4-((9-cyclopentyl-8-(phenylamino)-9H-purin-2-yl)amino)ph-en-yl)piperazin-1-yl)ethoxy)ethoxy)ethoxy)ethyl)(methyl)amino)-N-(2-(2,6-dioxopiperidin-3-yl)-1-oxoisindolin-4-yl)acetamide (**P6**)

Compound **P6** was prepared similarly as described for **P5**. Yellow solid, 28% yield, ¹H NMR (400 MHz, DMSO-*d*₆) δ 11.03 (s, 1H), 9.71 (s, 1H), 9.02 (s, 1H), 8.98 (s, 1H), 8.35 (s, 1H), 7.83 (t, *J* = 8.1 Hz, 3H), 7.61 (d, *J* = 8.9 Hz, 2H), 7.57–7.47 (m, 2H), 7.33 (t, *J* = 7.9 Hz, 2H), 6.98 (t, *J* = 7.3 Hz, 1H), 6.86 (d, *J* = 9.0 Hz, 2H), 5.15 (dd, *J* = 13.2, 5.0 Hz, 1H), 5.01–4.85 (m, 1H), 4.39 (q, *J* = 17.3 Hz, 2H), 3.57 (t, *J* = 5.4 Hz, 2H), 3.53–3.48 (m, 6H), 3.44 (s, 4H), 3.24 (s, 2H), 3.03 (s, 4H), 2.97–2.87 (m, 1H), 2.68 (t, *J* = 5.5 Hz, 2H), 2.63 (s, 1H), 2.56 (s, 4H), 2.49–2.40 (m, 4H), 2.38 (s, 3H), 2.02 (s, 6H), 1.75–1.63 (m, 2H). ¹³C NMR (100 MHz, DMSO-*d*₆) δ 173.3, 171.5, 169.6, 168.3, 154.9, 152.9, 149.6, 145.9, 143.3, 140.9, 134.5, 134.3, 133.7, 133.1, 129.2, 129.1 (2C), 127.4, 125.9, 122.0, 119.8, 119.7 (2C), 118.9 (2C), 116.4 (2C), 70.2 (2C), 70.1, 70.1, 68.8, 68.7, 61.5, 57.6, 56.9, 54.8, 53.7 (2C), 52.0, 49.7 (2C), 46.71, 43.4, 31.7, 29.5 (2C), 24.9 (2C), 23.0. HRMS (ESI): *m/z* calcd for C₅₀H₆₃N₁₂O₇: 943.49427 [M+H]⁺; found: 943.49047.

4.1.24. 2-(2-(2-(2-(2-(2-(4-(4-((9-cyclopentyl-8-(phenylamino)-9H-purin-2-yl)amino)-phenyl)piperazin-1-yl)ethoxy)ethoxy)ethoxy)ethoxy)ethyl)(methyl)amino)-N-(2-(2,6-dioxopiperidin-3-yl)-1-oxoisindolin-4-yl)acetamide (**P7**)

Compound **P7** was prepared similarly as described for **P6**. Yellow solid, 28% yield, ¹H NMR (400 MHz, DMSO-*d*₆) δ 11.03 (s, 1H), 9.73 (s, 1H), 9.04 (s, 1H), 8.99 (s, 1H), 8.35 (s, 1H), 7.83 (dd, *J* = 6.9, 4.6 Hz, 3H), 7.62 (d, *J* = 8.9 Hz, 2H), 7.56–7.48 (m, 2H), 7.33 (t, *J* = 7.9 Hz, 2H), 6.98 (t, *J* = 7.3 Hz, 1H), 6.87 (d, *J* = 9.0 Hz, 2H), 5.15 (dd, *J* = 13.3, 5.1 Hz, 1H), 5.02–4.91 (m, 1H), 4.38 (q, *J* = 17.3 Hz, 2H), 3.57 (t, *J* = 5.4 Hz, 4H), 3.52–3.47 (m, 8H), 3.44 (s, 4H), 3.26 (s, 2H), 3.08 (s, 4H), 2.97–2.86 (m, 1H), 2.74–2.58 (m, 9H), 2.48–2.42 (m, 2H), 2.39 (s, 3H), 2.02 (s, 6H), 1.75–1.63 (m, 2H). ¹³C NMR (100 MHz, DMSO-*d*₆) δ 173.3, 171.5, 169.5, 168.3, 154.9, 152.9, 149.6, 145.7,

143.3, 140.9, 134.5, 134.5, 133.7, 133.1, 129.2, 129.1 (2C), 127.4, 125.9, 122.0, 119.8, 119.6 (2C), 118.9 (2C), 116.5 (2C), 70.2, 70.2 (4C), 70.1, 70.1, 68.8, 61.4, 57.3, 56.9 (2C), 54.8, 53.4, 52.0 (2C), 49.3, 46.7, 43.4, 31.7, 29.5 (2C), 24.9 (2C), 23.0. HRMS (ESI): *m/z* calcd for C₅₂H₆₇N₁₂O₈: 987.52048 [M+H]⁺; found: 987.51632.

4.1.25. (2*S*,4*R*)-1-((*S*)-2-((2-(2-(2-(4-(4-((9-cyclopentyl-8-(phenylamino)-9H-purin-2-yl)amino)phenyl)piperazin-1-yl)ethoxy)ethoxy)ethyl)amino)-3,3-dimethylbutanoyl)-4-hydroxy-N-(4-(4-methylthiazol-5-yl)benzyl)pyrrolidine-2-carboxamide (**P8**)

VHL-L (0.25 g, 0.58 mmol), (ethane-1,2-diyl)bis (oxy)bis (ethane-2,1-diyl) bis(4-methylbenzenesulfonate) (0.53 g, 1.16 mmol), K₂CO₃ (0.16 g, 1.16 mmol), NaI (0.0348 g, 0.23 mmol) and CH₃CN (25 mL) were mixed in a flask. The resulted suspension was heated at 80 °C in an oil bath for 48 h. The solvent was evaporated under vacuum and the residue was isolated using column chromatography (DCM:MeOH = 40:1–20:1) to give compound **13a** as colorless oil. 33% yield, MS (ESI): *m/z* calcd for C₃₅H₄₉N₄O₈S₂: 717.3 [M+H]⁺; found: 717.5.

To a solution of **13a** (0.15 g, 0.21 mmol) in CH₃CN were added **6** (0.12 g, 0.27 mmol), K₂CO₃ (0.06 g, 0.42 mmol) and NaI (0.0126 g, 0.084 mmol). The resulted suspension was heated at 65 °C in an oil bath for 24 h. The solvent was evaporated under vacuum, and the residue was purified using column chromatography (DCM:MeOH = 20:1–10:1) followed by wash with PE:EA (10:1) to give compound **P8**. Yellow solid, 57% yield, ¹H NMR (400 MHz, DMSO-*d*₆) δ 9.03 (s, 1H), 8.98 (d, *J* = 8.8 Hz, 2H), 8.59 (d, *J* = 5.4 Hz, 1H), 8.36 (s, 1H), 7.83 (d, *J* = 7.9 Hz, 2H), 7.62 (d, *J* = 8.4 Hz, 2H), 7.47–7.37 (m, 4H), 7.33 (t, *J* = 7.7 Hz, 2H), 6.98 (t, *J* = 7.2 Hz, 1H), 6.87 (d, *J* = 8.7 Hz, 2H), 5.09 (s, 1H), 5.02–4.90 (m, 1H), 4.61–4.51 (m, 1H), 4.45–4.33 (m, 2H), 4.33–4.22 (m, 1H), 3.70–3.60 (m, 2H), 3.58–3.47 (m, 8H), 3.24 (s, 1H), 3.17 (s, 1H), 3.06 (s, 4H), 2.63 (s, 6H), 2.47–2.42 (m, 5H), 2.04 (s, 6H), 1.96–1.88 (m, 1H), 1.68 (s, 3H), 0.94 (s, 9H). ¹³C NMR (100 MHz, DMSO-*d*₆) δ 172.7, 172.5, 154.9, 152.9, 151.9, 149.6, 148.2, 145.8, 143.3, 140.9, 140.0, 134.4, 131.6, 130.1, 129.1 (2C), 129.1 (2C), 127.9 (2C), 127.4, 122.0, 119.6 (2C), 118.9 (2C), 116.5 (2C), 70.9, 70.1, 70.1, 69.4, 68.5, 66.8, 59.0, 57.6, 56.7, 54.8, 53.6 (2C), 49.5 (2C), 48.2, 42.1, 38.2, 35.4, 29.5 (2C), 27.0 (3C), 24.9 (2C), 16.4. HRMS (ESI): *m/z* calcd for C₅₄H₇₁N₁₂O₅S: 999.53911 [M+H]⁺; found: 999.53746.

4.1.26. (2*S*,4*R*)-1-((*S*)-2-((2-(2-(2-(2-(4-(4-((9-cyclopentyl-8-(phenylamino)-9H-purin-2-yl)amino)phenyl)piperazin-1-yl)ethoxy)ethoxy)ethyl)amino)-3,3-dimethylbutanoyl)-4-hydroxy-N-(4-(4-methylthiazol-5-yl)benzyl)pyrrolidine-2-carboxamide (**P9**)

Compound **P9** was prepared similarly as described for **P8**. Yellow solid, 28% yield, ¹H NMR (400 MHz, DMSO-*d*₆) δ 9.02 (s, 1H), 8.98 (d, *J* = 5.0 Hz, 2H), 8.58 (t, *J* = 5.7 Hz, 1H), 8.35 (s, 1H), 7.82 (d, *J* = 8.0 Hz, 2H), 7.62 (d, *J* = 8.7 Hz, 2H), 7.46–7.37 (m, 4H), 7.33 (t, *J* = 7.9 Hz, 2H), 6.98 (t, *J* = 7.3 Hz, 1H), 6.86 (d, *J* = 8.8 Hz, 2H), 5.07 (s, 1H), 5.01–4.90 (m, 1H), 4.62–4.50 (m, 1H), 4.45–4.33 (m, 2H), 4.33–4.20 (m, 1H), 3.72–3.59 (m, 2H), 3.58–3.42 (m, 14H), 3.23 (s, 1H), 3.12 (s, 1H), 3.04 (s, 4H), 2.59 (s, 4H), 2.54 (s, 2H), 2.48–2.40 (m, 5H), 2.02 (s, 5H), 1.97–1.87 (m, 1H), 1.69 (s, 2H), 0.92 (s, 9H). ¹³C NMR (100 MHz, DMSO-*d*₆) δ 173.4, 172.6, 154.9, 152.9, 151.9, 149.6, 148.2, 145.9, 143.3, 140.9, 140.0, 134.3, 131.6, 130.1, 129.1 (2C), 129.1 (2C), 127.9 (2C), 127.4, 122.0, 119.6 (2C), 118.9 (2C), 116.4 (2C), 71.0, 70.2, 70.2, 70.1, 69.4, 68.7, 66.8, 59.0, 57.6, 56.6, 54.8, 53.6 (2C), 49.6 (2C), 48.2, 42.1, 38.2, 35.4, 29.5 (2C), 27.0 (3C), 24.9 (2C), 16.4. HRMS (ESI): *m/z* calcd for C₅₆H₇₅N₁₂O₆S: 1043.56532 [M+H]⁺; found: 1043.56471.

4.1.27. (2*S*,4*R*)-1-((*S*)-2-((2-(2-(2-(2-(4-(4-((9-cyclopentyl-8-(phenylamino)-9*H*-purin-2-yl)amino)phenyl)piperazin-1-yl)ethoxy)ethoxy)ethoxy)ethyl)amino)-3,3-dimethylbutanoyl)-4-hydroxy-*N*-(4-(4-methylthiazol-5-yl)benzyl)pyrrolidine-2-carboxamide (**P10**)

Compound **P10** was prepared similarly as described for **P8**. Yellow solid, 36% yield, ¹H NMR (400 MHz, DMSO-*d*₆) δ 9.03 (s, 1H), 8.98 (d, *J* = 6.0 Hz, 2H), 8.59 (t, *J* = 5.7 Hz, 1H), 8.36 (s, 1H), 7.83 (d, *J* = 8.0 Hz, 2H), 7.62 (d, *J* = 8.9 Hz, 2H), 7.45–7.37 (m, 4H), 7.33 (t, *J* = 7.9 Hz, 2H), 6.98 (t, *J* = 7.3 Hz, 1H), 6.87 (d, *J* = 8.9 Hz, 2H), 5.08 (s, 1H), 5.03–4.88 (m, 1H), 4.62–4.52 (m, 1H), 4.46–4.33 (m, 2H), 4.32–4.20 (m, 1H), 3.70–3.62 (m, 2H), 3.61–3.47 (m, 16H), 3.47–3.44 (m, 2H), 3.25–3.20 (m, 1H), 3.17 (s, 1H), 3.07 (s, 4H), 2.65 (s, 6H), 2.48–2.40 (m, 5H), 2.04 (s, 5H), 1.96–1.87 (m, 1H), 1.78–1.63 (m, 2H), 0.93 (s, 9H). ¹³C NMR (100 MHz, DMSO-*d*₆) δ 172.7, 172.5, 154.9, 152.9, 151.9, 149.6, 148.2, 145.8, 143.3, 140.9, 140.0, 134.4, 131.6, 130.1, 129.1 (2C), 129.1 (2C), 127.9 (2C), 127.4, 122.0, 119.6 (2C), 118.9 (2C), 116.5 (2C), 70.9, 70.3 (3C), 70.2, 70.1 (2C), 69.4, 68.4, 66.8, 59.0, 57.5, 56.7, 54.8, 53.5 (2C), 49.4 (2C), 48.1, 42.1, 38.2, 35.4, 29.5 (2C), 27.0 (3C), 24.9 (2C), 16.4. HRMS (ESI): *m/z* calcd for C₅₈H₇₉N₁₂O₇S: 1087.59154 [M+H]⁺; found: 1087.58916.

4.1.28. (2*S*,4*S*)-1-((*S*)-2-(7-(4-(4-((9-cyclopentyl-8-(phenylamino)-9*H*-purin-2-yl)amino)phenyl)piperazin-1-yl)heptanamido)-3,3-dimethylbutanoyl)-4-hydroxy-*N*-(4-(4-methylthiazol-5-yl)benzyl)pyrrolidine-2-carboxamide (**P11**)

Compound **P11** was prepared similarly as described for **P1** using **VHL-L** as E3-recruitment element. Yellow solid, 30% yield, ¹H NMR (400 MHz, DMSO-*d*₆) δ 9.12 (s, 1H), 9.00 (d, *J* = 11.7 Hz, 2H), 8.67 (s, 1H), 8.36 (s, 1H), 7.85 (s, 3H), 7.65 (s, 2H), 7.41 (s, 4H), 7.32 (s, 2H), 6.98 (s, 1H), 6.89 (s, 2H), 5.47 (s, 1H), 5.01 (s, 1H), 4.53–4.36 (m, 2H), 4.32–4.15 (m, 2H), 3.96 (s, 1H), 3.45 (s, 2H), 3.16 (s, 4H), 3.06 (s, 2H), 2.80 (s, 4H), 2.45 (s, 5H), 2.34 (s, 1H), 2.24 (s, 1H), 2.04 (s, 5H), 1.91 (s, 1H), 1.69 (s, 2H), 1.52 (s, 4H), 1.27 (s, 4H), 0.97 (s, 9H). MS (ESI): *m/z* calcd for C₅₅H₇₁N₁₂O₄S: 995.5 [M+H]⁺; found: 995.5.

4.2. Biology

4.2.1. Cell lines and agents

HCC827, A549 and H1975 cells were provided by Stem Cell Bank, Chinese Academy of Sciences. HCC827 cell line were culture in RPMI-1640 supplemented with 10% heat inactivated fetal bovine serum (FBS), 1% sodium pyruvate, 1% glutamine and 1% penicillin-streptomycin. H1975 cell line were cultured in RPMI-1640 supplemented with 10% heat inactivated fetal bovine serum (FBS) and 1% penicillin-streptomycin. A549 were cultured in DMEM supplemented with 10% heat inactivated fetal bovine serum (FBS) and 1% penicillin-streptomycin. All cells were cultured in a humidified atmosphere containing 5% CO₂ at 37 °C.

MLN4924 (S7109) was purchased from Selleck. MG132 (M832899-5 mg) and Chloroquine (B20714-50 mg) were purchased from Macklin. Rapamycin (C843545-20 mg) was obtained from Shang Hai Yuan Ye.

4.2.2. Cell proliferation inhibition assay

The anti-proliferative activities of compounds against tumor cells were determined by MTT assay. Cells (3000–8000/well) were seeded in 96-well plates (200 μL medium/well) and incubated for 24 h. And the cells were treated with a series of concentrations of compounds and incubated for further 72 h 20 μL of MTT solution (5 mg/mL in PBS) was added to each well and incubated for 4 h. The supernatant in each well was removed carefully, and 150 μL of DMSO was added. The optical density of each well was determined by Varioskan Flash Multimode Reader (Thermo scientific) at 490 nm or 570 nm wavelength.

4.2.3. Western blotting assay

Cells (0.5–1 × 10⁶/well) were seeded in 6-well plates and incubated for 24 h. Cells were treated with different concentrations of compounds for indicated time and lysed by lysis buffer (Beyotime) with protease and phosphatase inhibitors. The suspension was centrifuged at 12,000 rpm for 20 min, and the insoluble material was removed. Protein (about 15 μg) was separated by 8% SDS-PAGE and transferred to PVDF membranes (Millipore). After incubation with primary and secondary antibodies (Xi'an Zhuangzhi Biotechnology Co., Ltd.), Membranes were imaged by a ChemiDoc MP Imaging system (BIO-RAD) and organized with Image Lab software.

The antibodies against EGFR (4267, 1:1000), Akt (4691T, 1:1000), P-EGFR (3777, 1:1000) and P-Akt (4060T, 1:1000) were purchased from Cell Signaling. PP62 (ab109012, 1:1000) and LC3B (ab192890, 1:2000) were purchased from abcam. β-actin (20536-1-AP, 1:1000) was purchased from proteintech.

4.2.4. Cell apoptosis assay

Cells (0.5–1 × 10⁶/well) were seeded in 6-well plates and incubated for 24 h. And compounds at indicated concentrations were added. Having been incubated for further 48 h, cells were collected and disposed with an Annexin V-FITC apoptosis detection kit (Becton Dickinson) according to the instructions and apoptosis rate was determined by the Flow Cytometry.

4.2.5. Cell cycle assay

Cells (0.5–1 × 10⁶/well) were seeded into 6-well plates and incubated for 24 h. And compounds at indicated concentrations were added. Having been incubated for further 48 h, cells were collected and washed twice with PBS. Cold ethanol (75%, 1.5 mL) was added dropwise and the cells were fixed at 4 °C for 20 h. The samples were centrifuged at 5000 rpm, and the supernatant was discarded completely. And the collected cells were treated with 500 μL PI/RNase (Becton Dickinson, #550825), incubated at 37 °C for 15 min and analyzed on a FACS Calibur™ flow cytometer (Becton Dickinson).

4.2.6. Cell colony formation assay

Cells (200/well) were seeded into 6-well plates and incubated for 24 h. And compounds at indicated concentrations were added. Having been incubated for 15 days, the cells were washed with PBS three times and fixed with cold ethanol (75%, 1.5 mL/well). The ethanol was removed followed by addition of crystal violet solution (0.1% in water) and incubation for 1 h. Colony number was counted and the photos were taken by a camera.

4.2.7. Statistical analysis

Data was analyzed using GraphPad Prism 5.0. DC₅₀ (concentration that caused deletion of 50% of EGFR) and IC₅₀ (concentration that resulted in 50% of cell growth inhibition) were calculated through the nonlinear regression-“log (inhibitor) vs response” analytical protocol. Statistical test was performed through “t tests (and nonparametric tests, **P* < 0.05, ***P* < 0.01, ****P* < 0.001)”.

Declaration of competing interest

The authors declare that they have no known competing financial interests or personal relationships that could have appeared to influence the work reported in this paper.

Acknowledgement

The financial support from The National Natural Science Foundation of China (Grant No. 81673354) is gratefully acknowledged.

Appendix A. Supplementary data

Supplementary data to this article can be found online at <https://doi.org/10.1016/j.ejmech.2020.112781>.

References

- [1] T.S. Mok, Y.-L. Wu, S. Thongprasert, C.-H. Yang, D.-T. Chu, N. Saijo, P. Sunpawaravong, B. Han, B. Margono, Y. Ichinose, Y. Nishiwaki, Y. Ohe, J.-J. Yang, B. Chewaskulyong, H. Jiang, E.L. Duffield, C.L. Watkins, A.A. Armour, M. Fukuoka, Gefitinib or carboplatin–paclitaxel in pulmonary adenocarcinoma, *N. Engl. J. Med.* 361 (2009) 947–957.
- [2] H.A. Yu, M.E. Arcila, N. Rekhtman, C.S. Sima, M.F. Zakowski, W. Pao, M.G. Kris, V.A. Miller, M. Ladanyi, G.J. Riely, Analysis of tumor specimens at the time of acquired resistance to EGFR-TKI therapy in 155 patients with EGFR-mutant lung cancers, *Clin. Canc. Res.* 19 (2013) 2240–2247.
- [3] M.L. Sos, H.B. Rode, S. Heynck, M. Peifer, F. Fischer, S. Klüter, V.G. Pawar, C. Reuter, J.M. Heuckmann, J. Weiss, L. Ruddigkeit, M. Rabiller, M. Koker, J.R. Simard, M. Getlik, Y. Yuza, T.H. Chen, H. Greulich, R.K. Thomas, D. Rauh, Chemogenomic profiling provides insights into the limited activity of irreversible EGFR inhibitors in tumor cells expressing the T790M EGFR resistance mutation, *Canc. Res.* 70 (2010) 868–874.
- [4] L. Chen, W. Fu, L. Zheng, Z. Liu, G. Liang, Recent progress of small-molecule epidermal growth factor receptor (EGFR) inhibitors against C797S resistance in non-small-cell lung cancer, *J. Med. Chem.* 61 (2018) 4290–4300.
- [5] K.S. Thress, C.P. Paweletz, E. Felip, B.C. Cho, D. Stetson, B. Dougherty, Z. Lai, A. Markovets, A. Vivancos, Y. Kuang, D. Ercan, S.E. Matthews, M. Cantarini, J.C. Barrett, P.A. Jänne, G.R. Oxnard, Acquired EGFR C797S mutation mediates resistance to AZD9291 in non-small cell lung cancer harboring EGFR T790M, *Nat. Med.* 21 (2015) 560–562.
- [6] M. Bersanelli, R. Minari, P. Bordi, L. Gnetti, C. Bozzetti, A. Squadrilli, C.A.M. Lagrasta, L. Bottarelli, G. Osipova, E. Capelletto, M. Mor, M. Tiseo, L718Q mutation as new mechanism of acquired resistance to AZD9291 in EGFR-mutated NSCLC, *J. Thorac. Oncol.* 11 (2016) e121–e123.
- [7] D. Zheng, M. Hu, Y. Bai, X. Zhu, X. Lu, C. Wu, J. Wang, L. Liu, Z. Wang, J. Ni, Z. Yang, J. Xu, EGFR G796D mutation mediates resistance to osimertinib, *Oncotarget* 8 (2017) 49671–49679.
- [8] S. An, L. Fu, Small-molecule PROTACs: an emerging and promising approach for the development of targeted therapy drugs, *EBioMedicine* 36 (2018) 553–562.
- [9] P.P. Chamberlain, L.G. Hamann, Development of targeted protein degradation therapeutics, *Nat. Chem. Biol.* 15 (2019) 937–944.
- [10] M. Scheepstra, K.F.W. Hekking, L. van Hijfte, R.H.A. Folmer, Bivalent ligands for protein degradation in drug discovery, *Comput. Struct. Biotechnol. J.* 17 (2019) 160–176.
- [11] I. Churcher, Protac-induced protein degradation in drug discovery: breaking the rules or just making new ones? *J. Med. Chem.* 61 (2018) 444–452.
- [12] P.M. Cromm, C.M. Crews, Targeted protein degradation: from chemical biology to drug discovery, *Cell Chem. Biol.* 24 (2017) 1181–1190.
- [13] M. Toure, C.M. Crews, Small-molecule PROTACs: new approaches to protein degradation, *Angew. Chem. Int. Ed.* 55 (2016) 1966–1973.
- [14] K.M. Sakamoto, K.B. Kim, A. Kumagai, F. Mercurio, C.M. Crews, R.J. Deshaies, Protacs: chimeric molecules that target proteins to the Skp1–Cullin–F box complex for ubiquitination and degradation, *Proc. Natl. Acad. Sci. Unit. States Am.* 98 (2001) 8554–8559.
- [15] N. Ohoka, K. Okuhira, M. Ito, K. Nagai, N. Shibata, T. Hattori, O. Ujikawa, K. Shimokawa, O. Sano, R. Koyama, H. Fujita, M. Teratani, H. Matsumoto, Y. Imaeda, H. Nara, N. Cho, M. Naito, In vivo knockdown of pathogenic proteins via specific and nongenetic inhibitor of apoptosis protein (IAP)-dependent protein erasers (SNIPERs), *J. Biol. Chem.* 292 (2017) 4556–4570.
- [16] M. Zengerle, K.-H. Chan, A. Ciulli, Selective small molecule induced degradation of the BET bromodomain protein BRD4, *ACS Chem. Biol.* 10 (2015) 1770–1777.
- [17] D. Remillard, D.L. Buckley, J. Paulk, G.L. Brien, M. Sonnett, H.-S. Seo, S. Dastjerdi, M. Wühr, S. Dhe-Paganon, S.A. Armstrong, J.E. Bradner, Degradation of the BAF complex factor BRD9 by heterobifunctional ligands, *Angew. Chem. Int. Ed.* 56 (2017) 5738–5743.
- [18] C. Qin, Y. Hu, B. Zhou, E. Fernandez-Salas, C.-Y. Yang, L. Liu, D. McEachern, S. Przybranowski, M. Wang, J. Stuckey, J. Meagher, L. Bai, Z. Chen, M. Lin, J. Yang, D.N. Ziazadeh, F. Xu, J. Hu, W. Xiang, L. Huang, S. Li, B. Wen, D. Sun, S. Wang, Discovery of QCA570 as an exceptionally potent and efficacious proteolysis targeting chimera (PROTAC) degrader of the bromodomain and extra-terminal (BET) proteins capable of inducing complete and durable tumor regression, *J. Med. Chem.* 61 (2018) 6685–6704.
- [19] V. Zoppi, S.J. Hughes, C. Maniaci, A. Testa, T. Gmaschitz, C. Wieshofer, M. Koegl, K.M. Ricking, D.L. Daniels, A. Spallarossa, A. Ciulli, Iterative design and optimization of initially inactive proteolysis targeting chimeras (PROTACs) identify VZ185 as a potent, fast, and selective von Hippel–Lindau (VHL) based dual degrader probe of BRD9 and BRD7, *J. Med. Chem.* 62 (2019) 699–726.
- [20] K. Raina, J. Lu, Y. Qian, M. Altieri, D. Gordon, A.M.K. Rossi, J. Wang, X. Chen, H. Dong, K. Siu, J.D. Winkler, A.P. Crew, C.M. Crews, K.G. Coleman, PROTAC-induced BET protein degradation as a therapy for castration-resistant prostate cancer, *Proc. Natl. Acad. Sci. Unit. States Am.* 113 (2016) 7124–7129.
- [21] G.E. Winter, D.L. Buckley, J. Paulk, J.M. Roberts, A. Souza, S. Dhe-Paganon, J.E. Bradner, Phthalimide conjugation as a strategy for in vivo target protein degradation, *Science* 348 (2015) 1376–1381.
- [22] H. Lebraud, D.J. Wright, C.N. Johnson, T.D. Heightman, Protein degradation by in-cell self-assembly of proteolysis targeting chimeras, *ACS Cent. Sci.* 2 (2016) 927–934.
- [23] B. Jiang, E.S. Wang, K.A. Donovan, Y. Liang, E.S. Fischer, T. Zhang, N.S. Gray, Development of dual and selective degraders of cyclin-dependent kinases 4 and 6, *Angew. Chem. Int. Ed.* 58 (2019) 6321–6326.
- [24] S. Rana, M. Bendjennat, S. Kour, H.M. King, S. Kizhake, M. Zahid, A. Natarajan, Selective degradation of CDK6 by a palbociclib based PROTAC, *Bioorg. Med. Chem. Lett* 29 (2019) 1375–1379.
- [25] C.M. Olson, B. Jiang, M.A. Erb, Y. Liang, Z.M. Doctor, Z. Zhang, T. Zhang, N. Kwiatkowski, M. Boukhali, J.L. Green, W. Haas, T. Nomanbhoy, E.S. Fischer, R.A. Young, J.E. Bradner, G.E. Winter, N.S. Gray, Pharmacological perturbation of CDK9 using selective CDK9 inhibition or degradation, *Nat. Chem. Biol.* 14 (2018) 163–170.
- [26] C.E. Powell, Y. Gao, L. Tan, K.A. Donovan, R.P. Nowak, A. Loehr, M. Bahcall, E.S. Fischer, P.A. Jänne, R.E. George, N.S. Gray, Chemically induced degradation of anaplastic lymphoma kinase (ALK), *J. Med. Chem.* 61 (2018) 4249–4255.
- [27] C. Zhang, X.-R. Han, X. Yang, B. Jiang, J. Liu, Y. Xiong, J. Jin, Proteolysis targeting chimeras (PROTACs) of anaplastic lymphoma kinase (ALK), *Eur. J. Med. Chem.* 151 (2018) 304–314.
- [28] M. Schapira, M.F. Calabrese, A.N. Bullock, C.M. Crews, Targeted protein degradation: expanding the toolbox, *Nat. Rev. Drug Discov.* 18 (2019) 949–963.
- [29] M.C. Silva, F.M. Ferguson, Q. Cai, K.A. Donovan, G. Nandi, D. Patnaik, T. Zhang, H.-T. Huang, D.E. Lucente, B.C. Dickerson, T.J. Mitchison, E.S. Fischer, N.S. Gray, S.J. Haggarty, Targeted degradation of aberrant tau in frontotemporal dementia patient-derived neuronal cell models, *eLife* 8 (2019), e45457.
- [30] A. Vogelmann, D. Robaa, W. Sippl, M. Jung, Proteolysis targeting chimeras (PROTACs) for epigenetics research, *Curr. Opin. Chem. Biol.* 57 (2020) 8–16.
- [31] J. Liu, J. Ma, Y. Liu, J. Xia, Y. Li, Z.P. Wang, W. Wei, PROTACs: a novel strategy for cancer therapy, *Semin. Canc. Biol.* (2020), <https://doi.org/10.1016/j.semcancer.2020.02.006>.
- [32] G.M. Burslem, A.R. Schultz, D.P. Bondeson, C.A. Eide, S.L. Savage Stevens, B.J. Druker, C.M. Crews, Targeting BCR-ABL1 in chronic myeloid leukemia by PROTAC-mediated targeted protein degradation, *Canc. Res.* 79 (2019) 4744–4753.
- [33] M. Xi, Y. Chen, H. Yang, H. Xu, K. Du, C. Wu, Y. Xu, L. Deng, X. Luo, L. Yu, Y. Wu, X. Gao, T. Cai, B. Chen, R. Shen, H. Sun, Small molecule PROTACs in targeted therapy: an emerging strategy to induce protein degradation, *Eur. J. Med. Chem.* 174 (2019) 159–180.
- [34] P. Ottis, C.M. Crews, Proteolysis-targeting chimeras: induced protein degradation as a therapeutic strategy, *ACS Chem. Biol.* 12 (2017) 892–898.
- [35] M. Zeng, Y. Xiong, N. Safaei, R.P. Nowak, K.A. Donovan, C.J. Yuan, B. Nabet, T.W. Gerro, F. Feru, L. Li, S. Gondi, L.J. Ombelets, C. Qian, P.A. Jänne, M. Kostic, D.A. Scott, K.D. Westover, E.S. Fischer, N.S. Gray, Exploring targeted degradation strategy for oncogenic KRAS^{G12C}, *Cell Chem. Biol.* 27 (2020) 19–31.
- [36] Y. Sun, X. Zhao, N. Ding, H. Gao, Y. Wu, Y. Yang, M. Zhao, J. Hwang, Y. Song, W. Liu, Y. Rao, PROTAC-induced BTK degradation as a novel therapy for mutated BTK C481S induced ibrutinib-resistant B-cell malignancies, *Cell Res.* 28 (2018) 779–781.
- [37] T. Neklesa, L. Snyder, R. Willard, N. Vitale, J. Pizzano, D. Gordon, M. Bookbinder, J. Macaluso, H. Dong, C. Ferraro, G. Wang, C. Crews, J. Houston, A. Crew, I. Taylor, ARV-110: an oral androgen receptor PROTAC degrader for prostate cancer, *J. Clin. Oncol.* 37 (2019), 259–259.
- [38] G.M. Burslem, B.E. Smith, A.C. Lai, S. Jaime-Figueroa, D.C. McQuaid, D.P. Bondeson, M. Toure, H. Dong, Y. Qian, J. Wang, A.P. Crew, J. Hines, C.M. Crews, The advantages of targeted protein degradation over inhibition: an RTK case study, *Cell Chem. Biol.* 25 (2018) 67–77.
- [39] M. Cheng, X. Yu, K. Lu, L. Xie, L. Wang, F. Meng, X. Han, X. Chen, J. Liu, Y. Xiong, J. Jin, Discovery of potent and selective epidermal growth factor receptor (EGFR) bifunctional small-molecule degraders, *J. Med. Chem.* 63 (2020) 1216–1232.
- [40] X. Zhang, F. Xu, L. Tong, T. Zhang, H. Xie, X. Lu, X. Ren, K. Ding, Design and synthesis of selective degraders of EGFR^{L858R/T790M} mutant, *Eur. J. Med. Chem.* 192 (2020), 112199.
- [41] H. Zhang, H.-Y. Zhao, X.-X. Xi, Y.-J. Liu, M. Xin, S. Mao, J.-J. Zhang, A.X. Lu, S.-Q. Zhang, Discovery of potent epidermal growth factor receptor (EGFR) degraders by proteolysis targeting chimera (PROTAC), *Eur. J. Med. Chem.* 189 (2020), 112061.
- [42] J. Yang, L.-J. Wang, J.-J. Liu, L. Zhong, R.-L. Zheng, Y. Xu, P. Ji, C.-H. Zhang, W.-J. Wang, X.-D. Lin, L.-L. Li, Y.-Q. Wei, S.-Y. Yang, Structural optimization and structure–activity relationships of N²-(4-(4-Methylpiperazin-1-yl)phenyl)-N⁸-phenyl-9H-purine-2,8-diamine derivatives, a new class of reversible kinase inhibitors targeting both EGFR-activating and resistance mutations, *J. Med. Chem.* 55 (2012) 10685–10699.
- [43] Y.-Y. Hei, Y. Shen, J. Wang, H. Zhang, H.-Y. Zhao, M. Xin, Y.-X. Cao, Y. Li, S.-

- Q. Zhang, Synthesis and evaluation of 2,9-disubstituted 8-phenylthio/phenylsulfinyl-9H-purine as new EGFR inhibitors, *Bioorg. Med. Chem.* 26 (2018) 2173–2185.
- [44] H. Lei, S. Fan, H. Zhang, Y.-J. Liu, Y.-Y. Hei, J.-J. Zhang, A.Q. Zheng, M. Xin, S.-Q. Zhang, Discovery of novel 9-heterocyclyl substituted 9H-purines as L858R/T790M/C797S mutant EGFR tyrosine kinase inhibitors, *Eur. J. Med. Chem.* 186 (2020), 111888.
- [45] X.-X. Xi, Y.-J. Liu, Y.-Y. Hei, M. Xin, L. Wang, S.-Q. Zhang, Synthesis and activity evaluation of EGFR double mutant inhibitors with the purine scaffold, *Chin. J. Med. Chem.* 30 (2020) 10–17.